Universitatea
Transilvania
din Brașov

INTERDISCIPLINARY DOCTORAL SCHOOL

Faculty of Construction

Eng. Ștefan-Ioan CÂMPEAN

THE STUDY OF THE NUCLEATION PHENOMENON IN THE ISOCHORIC ENVIRONMENT

ABSTRACT

Scientific supervisor,

Prof. habil. dr. ing. Gabriel NĂSTASE

Brașov, 2024

Contained

LIST NOTATIONS

TERM	NAME	UNIT OF MEASUREMENT
P	Pressure	[Pa]
V	Volume	[m3]
In	Mechanical work	[J]
T	Temperature	[K], [°C]
T	Time	[h]
m	Massage	[kg]
Z	Quality	[-]
$\mathcal{V}_0$	Specific volume	[m3/kg]
α	Coefficient of thermal expansion	[-]
β	Compressibility coefficient	[-]
A,B,C, Γ	Temperature and pressure functions	[-]
ϕ_1	Free Energy Relationship	[-]

DICTIONARY

TERM	EXPLANATION
Nucleation	The moment of transition from the liquid phase to the solid phase by changing the state of aggregation of a liquid

Izocor	Process or transformation into physical systems that take place at constant volume
Izobar	Process or transformation into physical systems that take place at constant pressure
Subcooling	The state of a substance, under physical conditions that would normally change its state of aggregation, but without causing this change
Supercooling	The state of a substance, under physical conditions that would normally change its state of aggregation, but without causing this change
Isochore nucleation	The phase transition of a substance in a constant volume environment.
Cryopreservation	Cold/frost preservation
Reactor izocor	Container resistant to high pressures, stable, non-deformable, with a well-defined volume in which substances that will be subjected to temperature changes can be placed
Reference temperature threshold	Temperature Level Control Point
Process of thermodynamics	Transition of a system in an equilibrium state to another equilibrium state
Thermodynamic equilibrium	Steady, balanced phase of a thermodynamic system
Meshing	Define a finite number of components that approximate an integer
Supercoold	Supercooling
Subcooled	Subcooling
Nucleation sites	Triggers of nucleation

1. CHAPTER 1: Introduction

People have been interested in the phenomenon of cooling since ancient times. Evidence of concerns about the use of cooling is available from the eleventh century BC, when the Chinese collected snow and ice that they stored in vaults and cellars and then used it during the hot period to cool drinks, food, or even the spaces in which they carried out their work [1] .

Similar concerns have also been discovered in Egypt, India (ca. 2000 BC) or during the period of the existence of the Roman Empire [1] . This trend has continued in recent history and we can remember the President of the United States of America, Thomas Jefferson who took the ice warehouse model from his travels in Europe and built an ice store in Monticello in the early 1800s, which he replenished with ice from nearby rivers or lakes in winter, and then use the ice for the warm season [2] .

Later in Mississippi, Dr. John Gorrie invented the first ice-making machine in 1845, but it was not until May 6, 1851 that Dr. Gorrie received the patent for his invention [3] . As the end of the century approached, keeping food and beverages cold became a necessity in the industry.

Gorrie's device had the ability to freeze a volume of water equivalent to a brick in about 2 hours [4] Figure 1.

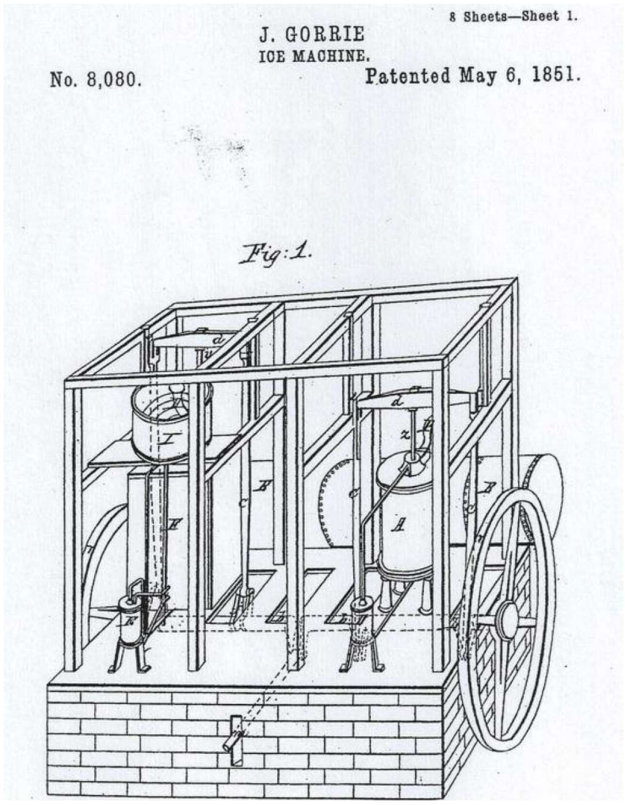

Figure 1 - Dr. John Gorrie's patented ice machine 1851 [3]

2. CHAPTER 2: Thermodynamic Processes

Thermotechnics is found at the intersection of mechanical and chemical engineering [5] . Thermodynamics is a branch of physics that deals with the macroscopic study of phenomena, in which a transfer of energy in the form of heat takes place, mechanical work, regardless of their nature. Its name is derived from the Greek language. [6]

How water behaves when cooled: up to a temperature of 4°C similar to other elements, it contracts and its density increases to the maximum level. Once with the temperature dropping below the limit of 4°C, the water begins to expand and implicitly its density decreases. Just below the 0°C threshold under natural conditions of constant atmospheric pressure and Water start toand change the aggregation state, the phenomenon of nucleation occurs, in isobaric regime, and the water passes from the liquid state ton solid state (ice). The density continues to decrease, this being and the reason why the ice rises at the surface of the water and floats. Further the graphic representation of the isobaric process in the natural environment, in Figure 2.

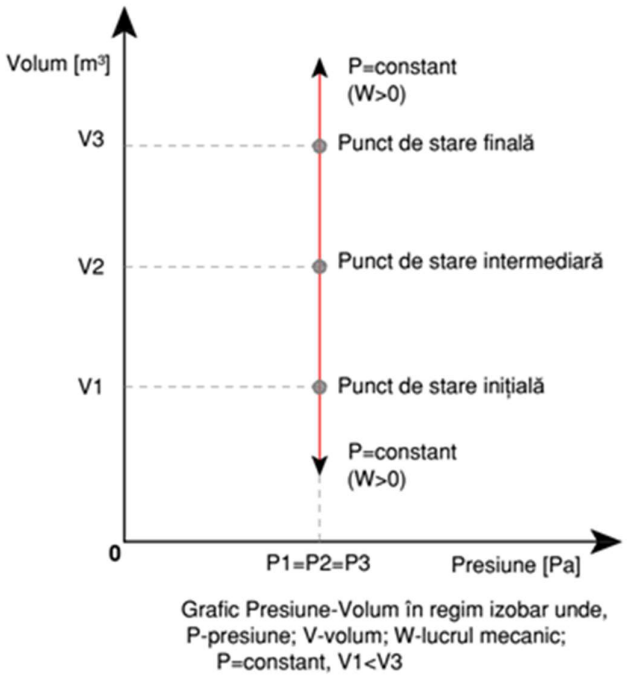

Figure 2 – Pressure-volume diagram in isobar regime

The behavior of a normal liquid as a function of temperature and volume can be represented by a curve Linear Figure 3A. It can be seen that the expansion quickly takes on proportions at very high temperatures.

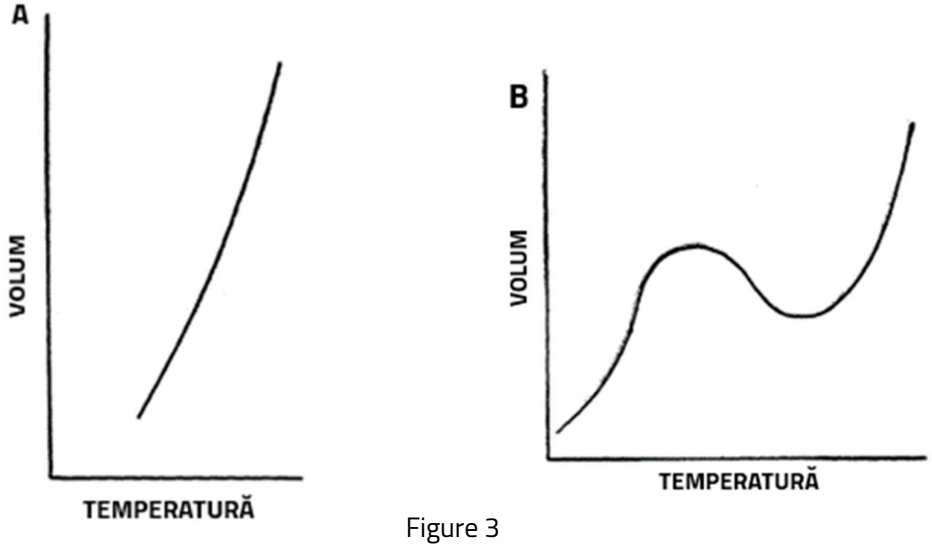

Figure 3

Fig. 3A Relationship between volume and temperature for a normal liquid Fig. 3B [7] The hypothetical relationship between volume and temperature for liquid water, if it were cooled indefinitely, without the appearance of the ice core [7]

These considerations lead us to study the curve for water in the form of the one presented in Figure 3B. It is important to mention that an increase in pressure would change the shape of the curve in Figure 3B in a linear model similar to Figure 3A [7] .

Studies and experiments have shown that water can be in a state of liquid aggregation, at normal pressure even at much lower temperatures. This phenomenon is in fact the metastable state of a substance which, although cooled below the temperature threshold to which it should have passed in the next state of aggregation, retains its initial state of aggregation.

This process of extreme subcooling requires the water to be in its pure form, without the existence of other micro particles that can play the role of nucleation triggers (the specific definition in English: "*nucleation sites*"), obtained by the technique of reverse osmosis or chemical demineralization. [8]

Following the measurements, the supercooled water was identified at a temperature of approximately - 41°C. This has been defined as *the homogeneous nucleation temperature* – being the lowest temperature at which the rate of crystallization of ice can be assessed as water freezes.

3. CHAPTER 3: The Isogate Environment and the Multiple Forms of Ice

Water in its solid form, called ice, is naturally found in the environment on Earth in the form of hexagonal crystals, called Ih ice. In very rare cases, the type of ice Ic has also been discovered, whose crystal shape is cubic and the temperature at which it forms is between -143 °C and -53 °C. It can exist up to -33 °C after which it turns into Ih ice [9] . These are the only forms of ice that are found on our planet naturally.

Up to twenty types of ice have been discovered so far.Apart from the common ice mentioned above, the rest were created under laboratory conditions as a result of extreme temperatures and pressures that are characteristic of an insulating environment [10] .

What would it be like if the environment in which the thermodynamic process takes place is modified by restricting the variability of volume? Basically, we have an airtight container, to which we apply temperature changes. Through heating or cooling the element inside the container, we will obtain the temperature variation, but The physical changes inside will be limited to the non-deformable volume of the container. We obtain a thermodynamic system in which the temperature varies, the pressure varies and the volume remains constant, and the mechanical work inside the container tends towards 0. This is how we can describe the isochore thermodynamic regime. Further it can be seen graphically in a diagram concept, Figure 4 :

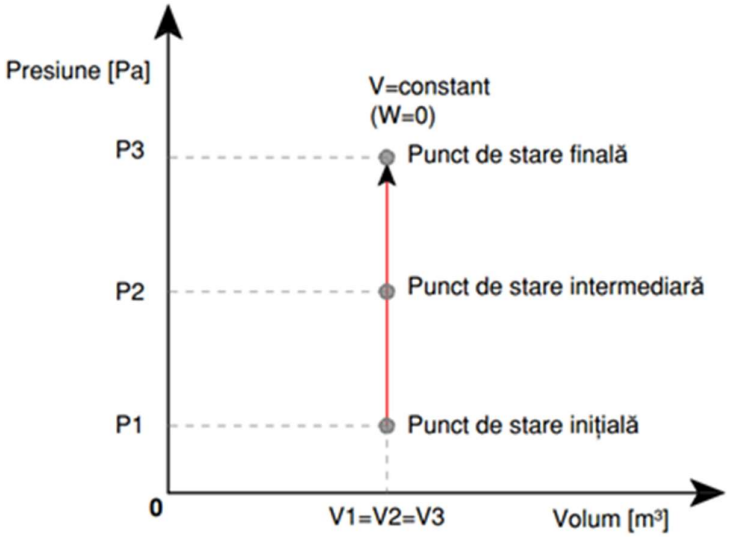

Grafic Presiune-Volum în regim izocor unde,
P-presiune; V-volum; W-lucrul mecanic;
V=constant, P1<P3

With the discovery of the principles of thermodynamics, it was possible to study these techniques of temperature variation in the isochore regime. Thus, the effect of high hydrostatic pressures was discovered, and the water phase diagram was discovered, which was published in 1912 by Percy Williams Bridgman. Along with this diagram, one of the triple points of water was published for the first time, which is reached at a temperature of -21.985 °C and a pressure of 209.9 MPa, when type Ih ice (the common type, the most widespread in nature, made up of hexagonal crystals), type III (tetragonal shaped crystals) and liquid coexist being in a state of thermodynamic equilibrium [7] .

In *Figure 5* you can see how P.W.Bridgman presents the existence of water in a phase Liquid and in five types of ice (ice I, II, III, IV, V). The types of ice are differentiated from each other by the conditions under which they are formed (temperature variations and pressure very different) [7] .

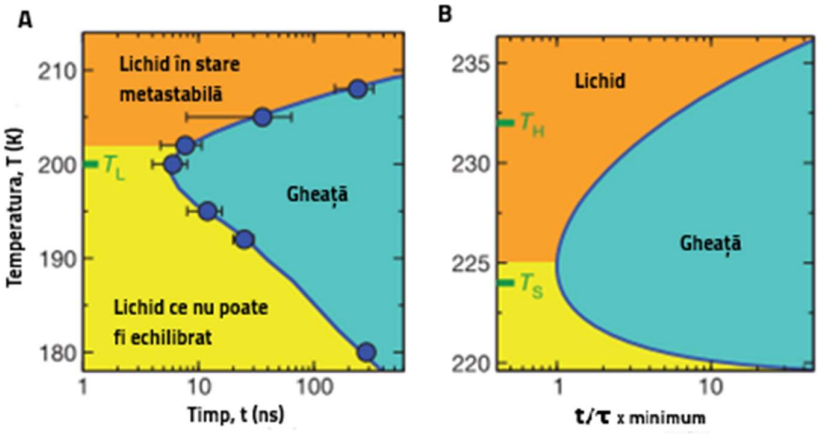

Figure 4 –Diagram pressure - volume in isochore regime:

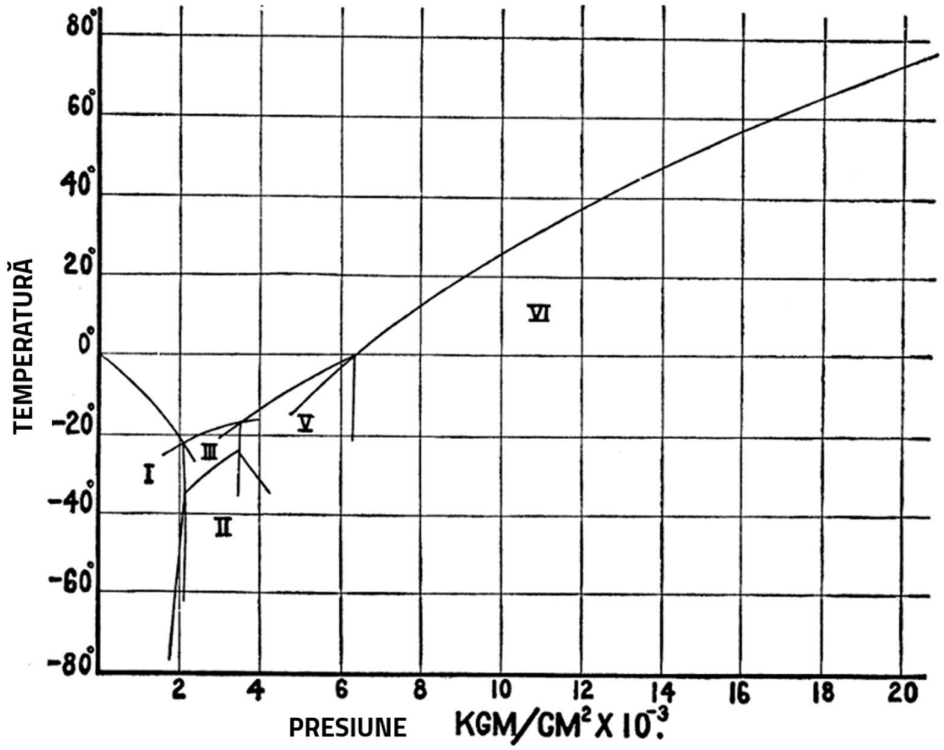

Figure 5 - Representation of equilibrium curves between ice I, II, III, IV, V and liquid [7]

In an isochore system, the volume of which remains constant, the ice cannot expand freely. Thus, as it is formed, in the system develops a hydrostatic pressure (*Figure 6*). It is observed that there was a pressurized system in two phases, with an unfrozen liquid portion and a solid portion ice cream coexisting at a temperature below the point of Frost of water. In practice, isochoric thermodynamic conditions can be achieved in any rigid container that can withstand high pressures [11] .

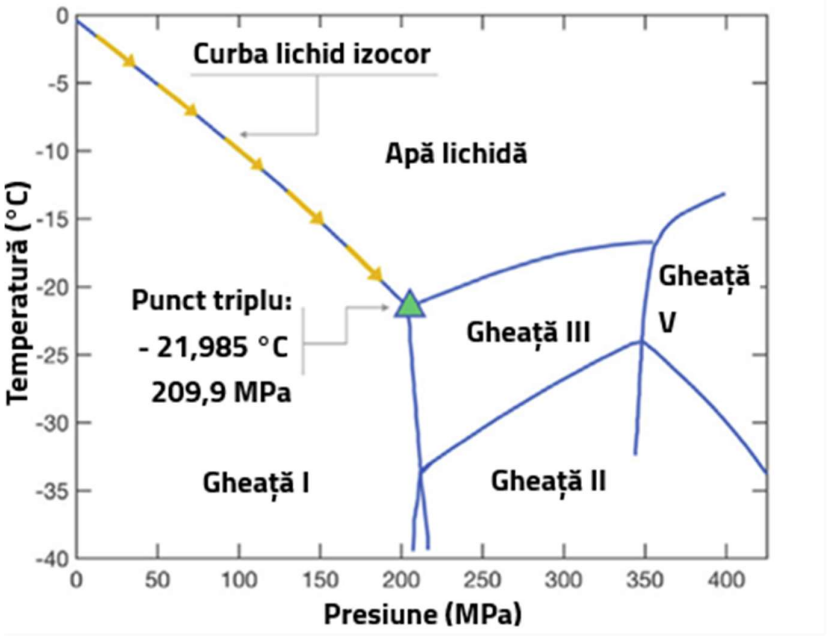

Figure 6 - Pure water phase diagram. The curve between liquid water, ice I, and ice III marks the equilibrium pressure that an isometric system experiences at a certain temperature below 0°C but higher than the triple-point temperature (-21.985°C) [12].

4. CHAPTER 4: Nucleation of water in isochore regime

The metastable state of water subcooling is a critical, unstable thermodynamic zone, which can be very easily unbalanced by external disturbances. When a disturbance in the system proves to be large enough, the phase change has passed the point from which it can no longer return [12] . The aforementioned disturbances actually trigger cavitation which is most responsible for the nucleation of ice, according to research over the last century. Even if [13] [14] the cavitation phenomenon is mainly associated with ultrasound, it can also be triggered from Faraday instability.

Firstly, the absence of air in the system restricts the cavitation that can be created in the air dissolved in water, and secondly, the formation of a low-density air bubblein a small volume of water will create a positive pressure due to Le Chatelier's principle, increasing its energy barrier of formation [12] .

Because the density of Ih type ice is lower than the density of water, the formation of an ice core in an isometric medium (constantly restricted volume) will cause an increase in pressure. The energy required to overcome such an increase in pressure makes homogeneous nucleation of ice thermodynamically unlikely in an isochorus system at temperatures above -109 °C [15] .

5. CHAPTER 5: Current state of research

Ice can nucleate from the supercooled liquid in two ways: homogeneous, when it is sufficiently cooled to conduct a spontaneous formation of the ice core (approximate temperature - 40°C) or heterogeneous, when there is a disturbance of foreign agents [16] (a foreign particle, a surface, air bubbles, etc.) that reduce the kinetic barrier [17] to the formation of the ice core and produce nucleation even at temperatures higher than -40°C. As a rule in isocore systems, the formation of the ice core is heterogeneous and occurs at first on the walls of the container.

These peculiarities motivated the creation of a device that can detect the metastable equilibrium state in antithesis to the nucleation of an isochoric system, with a volume greater than 1mL. It was called (INDe – *isochoric nucleation detector* - nucleation detector in isocor), and uses unique thermodynamic properties of isochore cooled water in containers of constant volume to detect with a latency low nucleation, [18] Figure 7

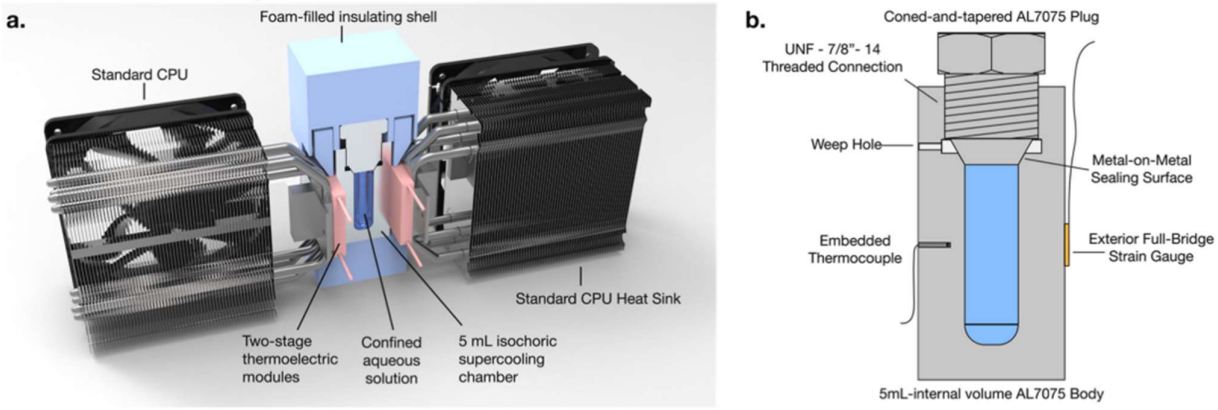

Figure 7 - Isochoric nucleation detection device (INDe). [25]

The high pressure inside produces a rapid and slight plastic deformation of the container (of negligible dimensions) which is immediately detected by the voltage sensor. It was seen by comparing the values that the two signals are almost identical, with a response time of less than one second, thus validating this a new way to detect the appearance of nucleation from within. [18]

In one of the most recent studies A microscope designed to be used in Visual studies in isochore experiments. Its name is: ISCM (*isochoric, supercooling cryomicroscope* – isochoric cryomicroscope with supercooling). Basically, a conventional microscope was attached to an isochoric container equipped with transparent elements through which the interior of the isochoric chamber can be visualized. The part is cooled with a refrigerant (water with ethylene glycol in a proportion of 50% each) which is introduced through the internal circuit of the device and the parameters controlled by means of a cooling equipment. The minimum operating temperature limit is – 22°C, *Figure 8* [19] .

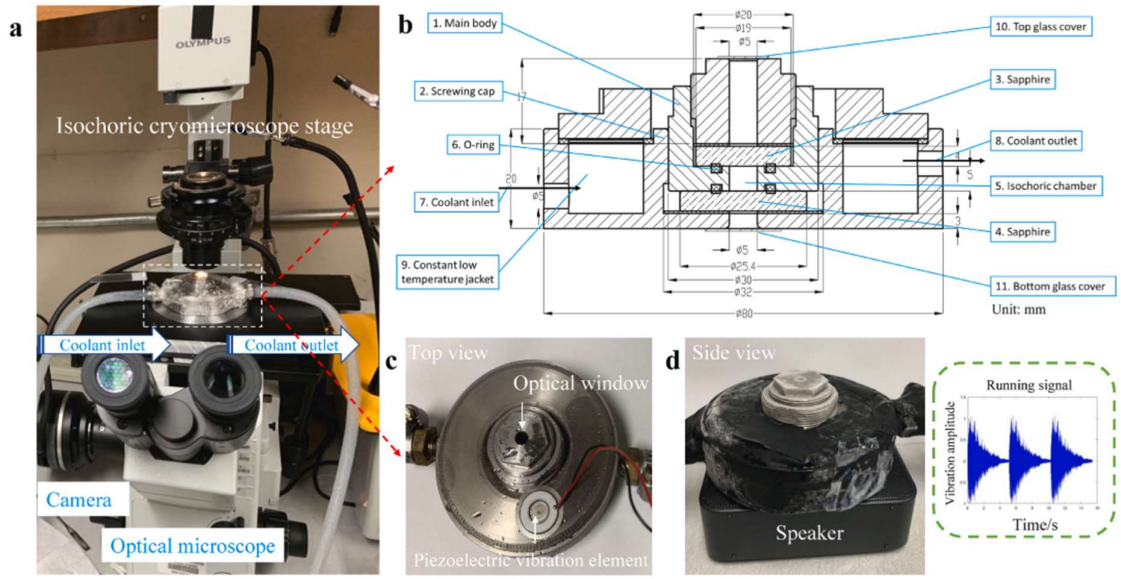

Figure 8 - Supercooled isochoric cryomicroscope (ISCM). a – ISCM system configuration, b – cross-section through the ISCM body, c – top view of the device, together with a piezoelectric vibrating element, d – side view of the ISCM placed on a diffuser with a disruptive role, favorable to nucleation.

The temperature at which the experiments were carried out was -5°C and the supercooling state was confirmed for both environments. In all cases for the isochore medium, the metastable state of supercooling was maintained regardless of the nature of the disturbances, while in the isobar medium they led to nucleation, Figure 9 . [19]

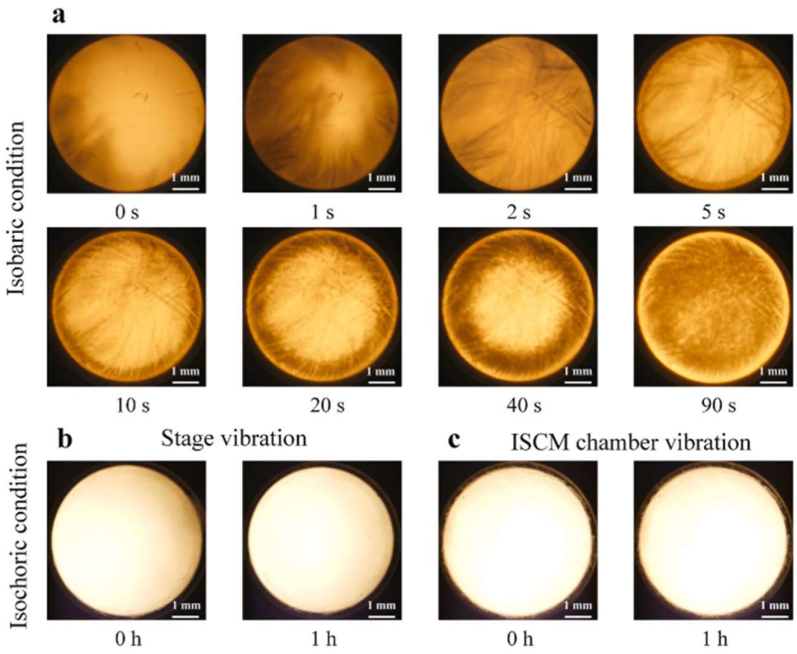

Figure 9 - Images of the comparative study between the stability of supercooled deionized water in the isobaric medium and in the isochore medium taken with ISCM. a – The process of ice formation and growth in the isobaric environment in an interval of 0-90 seconds. b, c – Absence of ice crystals for isochore conditions and mechanical disturbance [19] .

6. CHAPTER 6: The Mathematical-Physical Perspective of the Nucleation Phenomenon in the Isochoric Environment

6.1 Basics, system characterization

Through thermodynamic analysis, some mathematical models have been described that characterize the freezing process of water and aqueous solutions in a constant volume environment. The constant volume cooling process is characterized by a number of properties: [20]

- The process takes place in a two-phase thermodynamic system where the liquid coexists with the ice
- In a two-phase system, temperature and pressure are interdependent and influence each other
- The quality of the system is defined as the relative percentage of water and ice between which the isochore volume is divided
- Both the temperature or pressure and the quality of the system can fully specify the freezing process in an isochord system

The temperature at which the phase change occurs in a simple thermodynamic system that is based on a pure substance, being in a gravitational field, is a unique function of pressure. To be

more practical and easier, the regression curve defining the relationship between temperature and pressure has been defined at the phase change from liquid to the intersection with type Ih ice and type III ice. The equation that defines this curve is:

Equation 1 - pressure as a function of temperature at phase change

$$P = -0{,}1461 \cdot T^2 - 12{,}58 \cdot T + 0{,}1013 \quad (1)$$

Where: P - pressure in [Mpa];

T - temperature in [°C];

In order for an isochore system to be exemplified in mathematical physics terms, the mass percentage of water relative to the total mass of the mixture of water and ice, for a given point of temperature and pressure, will define the quality of the system. The term is denoted with the letter *Z*.

Equation 2 -Quality *Z* of the

$$Z = \frac{\mathcal{V}_0 - \mathcal{V}_1}{\mathcal{V}_2 - \mathcal{V}_1} \quad (2)$$

Where:

$\mathcal{V}_0$ – the specific volume under the initial conditions [m³/kg]

$\mathcal{V}_1$ – specific ice volume [m³/kg]

$\mathcal{V}_2$ – specific volume of water [m³/kg]

The specific volumes for ice and water as a function of temperature and pressure will be given in the following set of equations that have been defined in the paper: "Freezing processes in high-pressure domains," *International Journal of Refrigeration*, vol. 20, no. 5, pp. 301–307, 1997, doi: 10.1016/S0140-7007(97)00027-3 by P. D. Sanz, L. Otero, C. De Elvira, and J. A. Carrasco [21]

For the ice:

Equation 3 - Specific volume in the case of ice as a function of temperature - pressure [21]

$$\mathcal{V}_1 = \mathcal{V}_{10} \exp\left[-\int_{P0}^{P} \beta_{T1}(P', T)dP' + \int_{T0}^{T} \alpha_{T1}(P_0, T')dT'\right] \quad (3)$$

Where:

α - coefficient of thermal expansion

β – compressibility coefficient

0 – the index represents the state and properties of water at freezing temperature for water at atmospheric pressure (1 Atm or 101325 Pa)

$$\alpha_{T1}(P_0, T') = A_1 + A_2 T + A_3 T^2 + A_4 T^3 \quad (4)$$

$$\beta_{T1}(P', T) = \frac{\beta_{T1}^0}{1 + m_1 \beta_{T1}^0 P};\ \beta_{T1}^0 = \frac{\beta_1}{1 - \beta_2 T} \quad (5)$$

Where:

$A_1 = 1{,}5756 \cdot 10^{-4}$

$A_2 = 5{,}556 \cdot 10^{-7}$

$A_3 = 2{,}655 \cdot 10^{-8}$

$A_4 = 7{,}11 \cdot 10^{-10}$

$\beta_1 = 1{,}827 \cdot 10^{-5}$

$\beta_2 = 1{,}418 \cdot 10^{-3}$

$m_1 = 5$

P - pressure in [bar];

T - temperature in [°C];

For water:

Equation 4 - The specific volume in the case of water as a function of temperature – pressure [21]

$$\mathcal{V}_2 = \mathcal{V}_{10} \exp\left[- \int_{P0}^{P} \beta_{T2}(P', T) dP' + \int_{T_{k_0}}^{T_k} \alpha_{T2}(P_0, T') dT' \right] \quad (6)$$

Where:

$$\beta_{T2}(P, T) = \left(\sum_{i=0}^{4} b_i P^i \right) \cdot 10^{-4} \quad (7)$$

$$\alpha_{T2} = \left(A + \frac{B}{C + \Gamma} \right) \cdot 10^{-4} \quad (8)$$

And A, B, C, are temperature and pressure functions expressed as follows:Γ

$$A = a_1 + a_2 T_k + a_3 T_k^2 \quad (9)$$

$$B = a_4 + a_5 T_k + a_6 T_k^2 + a_7 T_k \Gamma + a_8 \Gamma \quad (10)$$

$$C = a_8 + a_9 T_k + a_{10} T_k^2 + a_{11} T_k^3 \quad (11)$$

$$\Gamma = P + a_{13} P^2 + a_{14} P^3 \quad (12)$$

The coefficients used in the expressions of temperature and pressure functions are:

$$a_1 = 4{,}7856 \cdot 10^{1}$$

$$a_2 = -\,8{,}12847 \cdot 10^{-2}$$

$$a_3 = 8{,}49849 \cdot 10^{-5}$$

$$a_4 = 5{,}56047 \cdot 10^{5}$$

$$a_5 = -3{,}76355 \cdot 10^{3}$$

$$a_6 = 5{,}56395$$

$$a_7 = 5{,}59682 \cdot 10^{-3}$$

$$a_8 = -2{,}76522 \cdot 10^{1}$$

$$a_9 = -4{,}28067 \cdot 10^{3}$$

$$a_{10} = -3{,}39150 \cdot 10^{1}$$

$$a_{11} = 3{,}65873 \cdot 10^{-1}$$

$$a_{12} = -5{,}89617 \cdot 10^{-4}$$

$$a_{13} = 3{,}28892 \cdot 10^{-4}$$

$$a_{14} = 2{,}65933 \cdot 10^{-8}$$

$$b_0 = 4{,}41753 \cdot 10^{-1}$$

$$b_1 = -1{,}09205 \cdot 10^{-4}$$

$$b_2 = 1{,}99785 \cdot 10^{-8}$$

$$b_3 = -2{,}08128 \cdot 10^{-1}$$

$$b_4 = 8{,}86050 \cdot 10^{-17}$$

Where : P - pressure in [bar];

T - temperature in [K];

The specific value of the volume of water can be calculated numerically using the above constants. The constants for water were taken from: *L. Ter Minassian, P. Pruzan, and A. Soulard, "Thermodynamic properties of water under pressure up to 5 kbar and between 28 and 120 °C. Estimations in the supercooled region down to -40 °C," J Chem Phys, vol. 75, no. 6, pp. 3064–3072, 1981, doi: 10.1063/1.442402* [22] .

7. CHAPTER 7:Modulation of the thermo-mechanical behavior of the isochoric visualization device by means of a computer simulation software

Through these simulations, we were able to identify potential problems and optimize in the design and development stages, reducing the costs and time required for physical testing.

7.1 Simulation results

The reference values regarding the tensile strength limits of the materials that make up the sight device for aluminum alloy 7075-T6 are 560 MPa and sapphire glass that reaches a maximum of 400 MPa at a temperature of 298 K or a minimum of 275 MPa around the temperature of 770 K [23] [24] .

The Von Mises voltage [N/m2] is graphically simulated in COMSOL and it is observed that the maximum value reaches 2.18 x 108 N/m2 i.e. 218 MPa for the internal pressure of 1200 bar, which is corresponding to the limit temperatures to which the device has been subjected. The most sensitive is the 400 MPa Al2O3 sapphire viewing glass and then the 560MPa 7075-T6 aluminum alloy. Both materials fit these values without problems. We also performed a simulation for the operating pressure of 2100 bar, which could be recorded at a triple water point temperature of -21.985°C. In this case, the values approach the maximum values of sapphire, reaching 391 MPa on the surface of the sapphire lens. Basically, the resistance is confirmed until the triple point of the water is reached. As can be seen in Figure 10 and Figure 11 The greatest pressure is focused on the lenses, which are also the most vulnerable. We can consider that the stress test has been successfully passed.

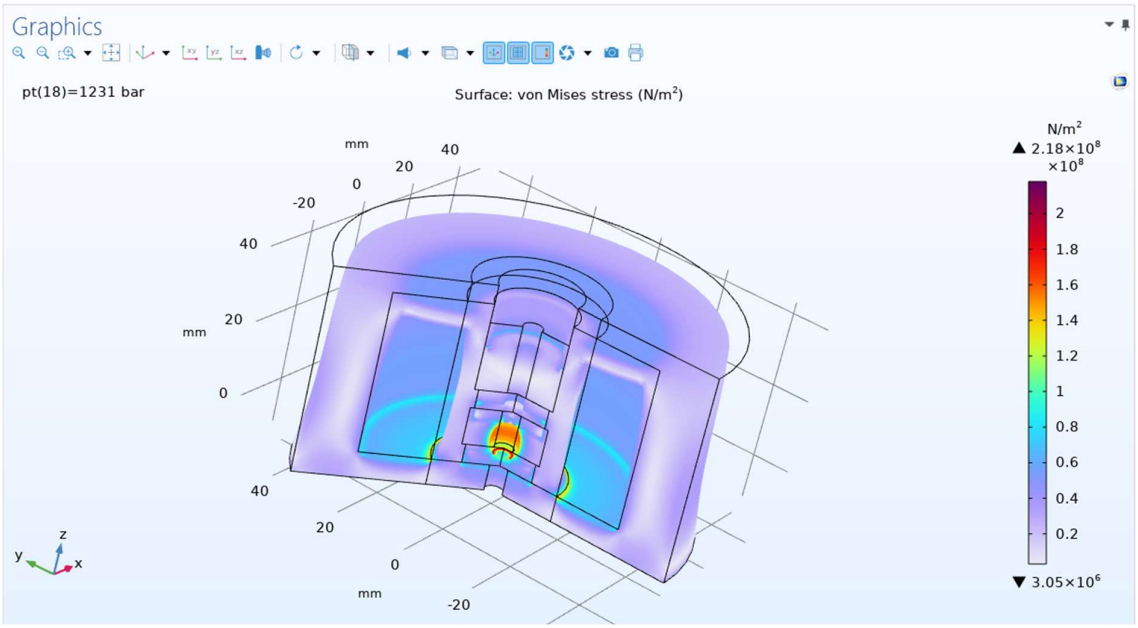

Figure 10 - Presentation of the Von Misses voltage N/m2 for a pressure of 1231 bar or 123.1 MPa, overview.

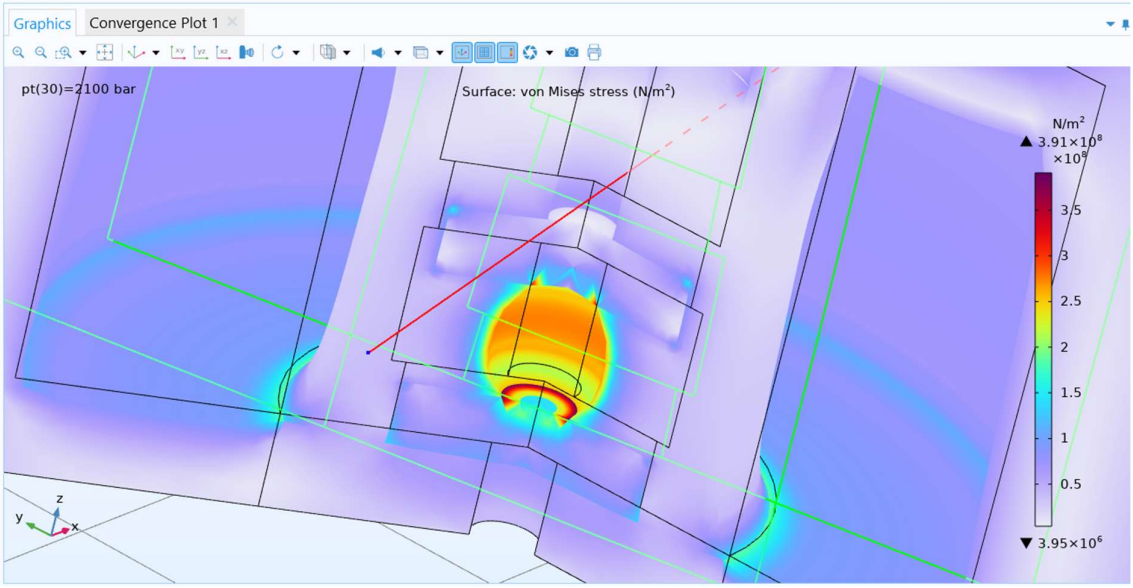

Figure 11 - Presentation of the Von Misses voltage N/m2 for a pressure of 2100 bar or 210MPa, near view.

The studied model was subjected to an internal pressure that corresponds to the temperature of almost -22°C. Thus, we have created a simulation model for the equilibrium temperature, and in the following figure you can see a simulation of the contour isotherms, Figure 12.

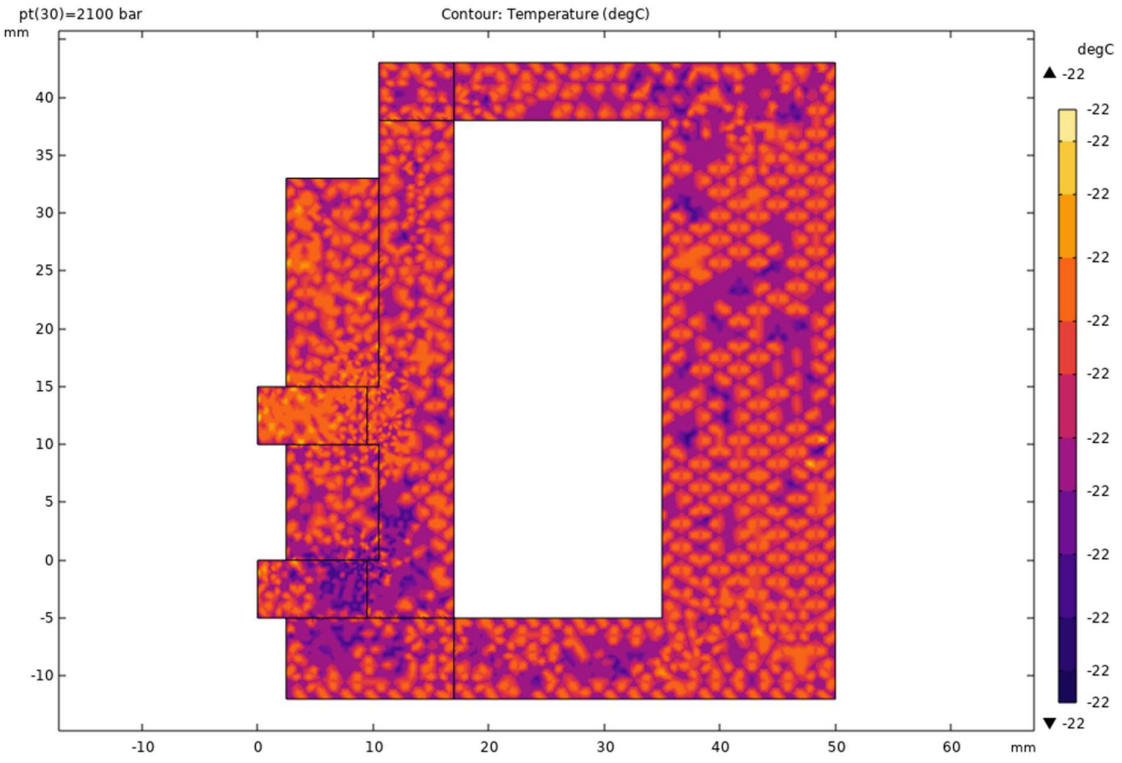

Figure 12 - Presentation of isotherms on the display device at -22°C and 2100 bar

According to the data obtained through the simulations in the resistance and heat transfer modules, we can conclude that the design of the device can move to the next stage, namely its implementation and the creation of a prototype for testing. Now that the aforementioned parameters have been tested in computer simulation, the resources for the physical realization of the device will be used at a much better yield.

7.2 Simulation of fluid flow

The isochoric viewing device is cooled by means of a cooling fluid (a mixture of distilled water and 50% glycol) that circulates through the cooling jacket surrounding the isochore chamber.

7.3 Simulation results

The way in which the pressure varies is further represented. We notice how the pressure is concentrated on the side wall of the isoporic chamber near the inlet connection, after which areas of lower pressure are created near the outer jacket, increasing again towards the exit area towards the return connection, and decreasing considerably in the return connection.

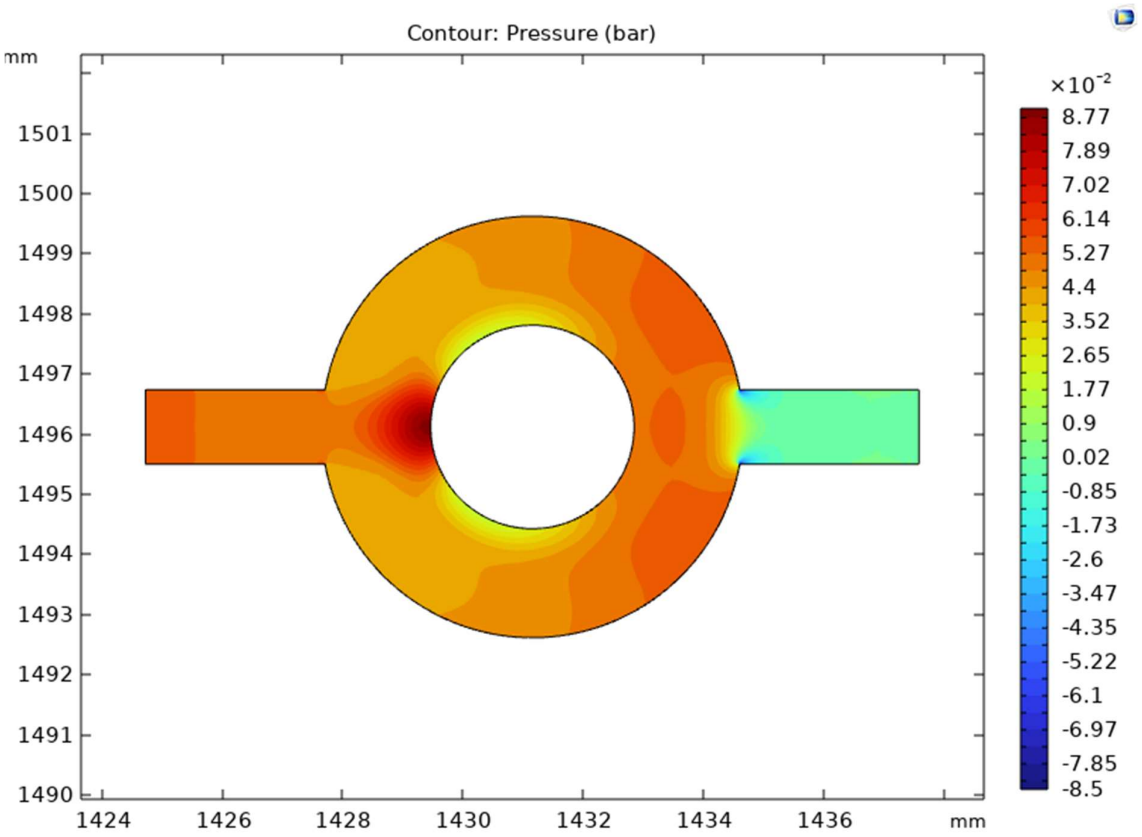

Figure 13 - Distribution of coolant pressures (thermal agent) inside the viewing device

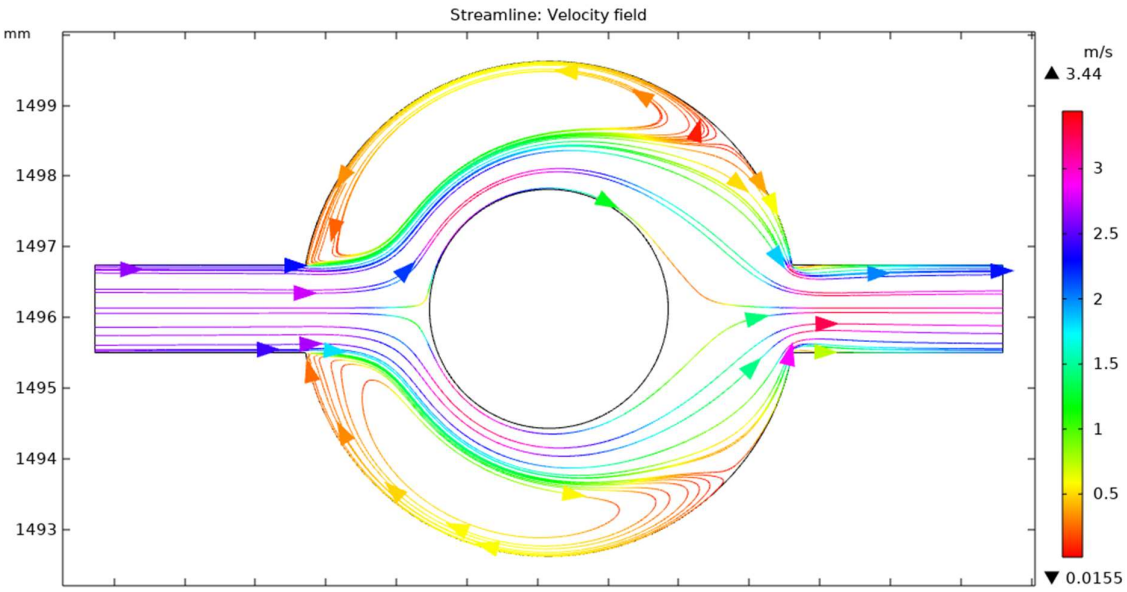

Figure 14 -Flow velocities and movement of the thermal agent inside the viewing device.

The flow inside the cooling jacket of the isochore chamber is a turbulent one, and its graphic representation was generated by COMSOL in Figure 14. It can be seen how the core creates a spinning effect of the coolant, creating on either side two areas where the speed drops to close to 0, having a stagnation effect in the outer areas of the cooling jacket. The velocity remains in the range of 1.5-2 m/s around the isochoric chamber, which will provide coolant in a continuous flow to control the internal temperature.

8. CHAPTER 8: Devices, Equipment, Methodology and Research Materials

The studies were carried out using the following devices and equipment:

8.1 High Pressure Isochoric Micro Reactor MS-1 type manufactured in the USA by HIP (High Pressure Equipment Company). The standard construction material is type 316 stainless steel. Operation at temperatures up to 425 °C is made possible by the construction of the metal-to-metal conical seal. The maximum pressure is at 410 MPa (HF4 construction). Further in Figure 15 The graphic model of the reactor is presented.

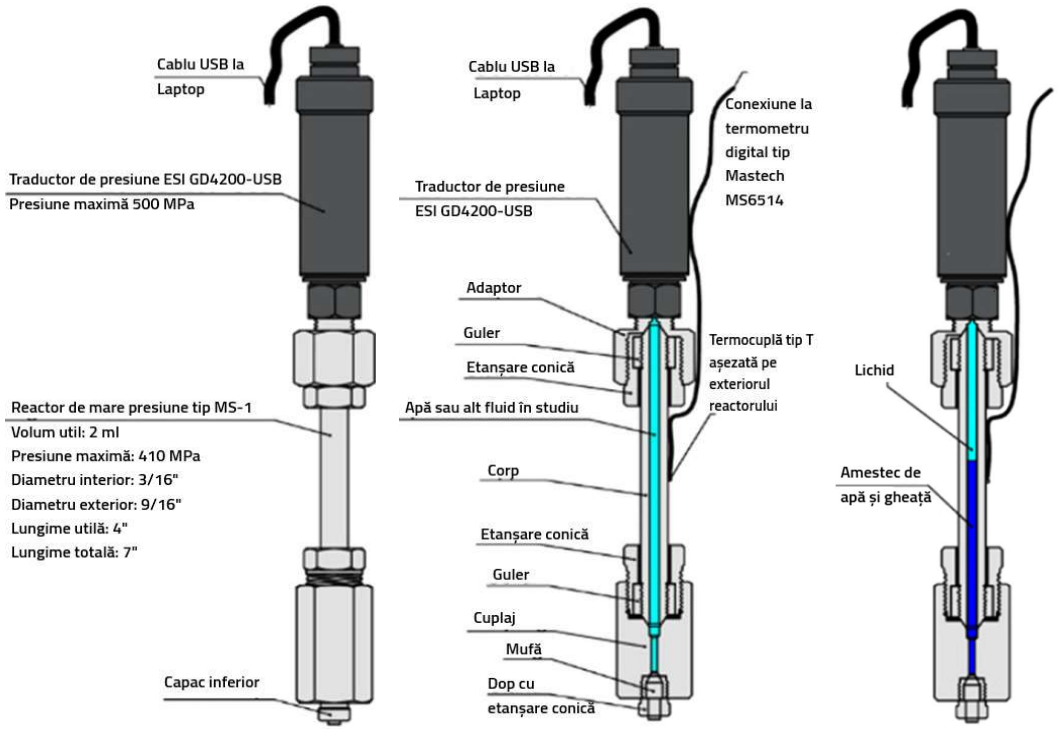

Figure 15 - High pressure reactor type MS-1 $V_{useful=}$ 2 ml, front view, pre-frost section and sub-0°C temperature section

8.2 Digital Pressure Transducer, GD4200-USB model manufactured in the UK by ESI Technology Ltd. Excellent measurement accuracy allows the user to measure any pressure that the application requires, from vacuum to 5,000 bar. The operating temperature is in the range of -50°C to +125°C for the measured environment, for an ambient temperature range of -20°C to +85°C. In Figure 16 you can see the image of the transducer and the accompanying USB cable.

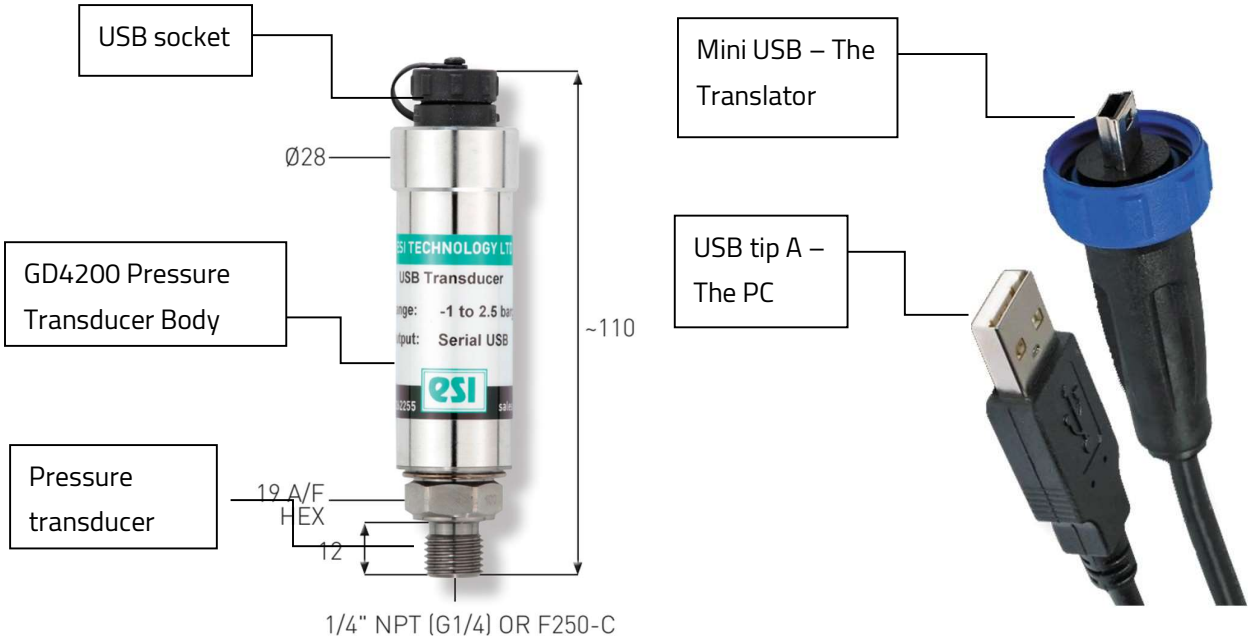

Figure 16 - ESI GD4200-USB pressure transducer and USB Type-A + mini USB cable and threaded coupling with moisture and water protection.

8.3 Thermocouple, the temperature is measured using one or two *T-type thermocouple* (specific for high-accuracy measurements in the refrigeration and cryogenic field). Repeatability is excellent in the range of -200°C to 200°C (±0.1°C). An example can be viewed in Figure 17. The thermocouples will be connected to a digital thermometer *Mastech MS6514* (produced by Digital Inc, China) that further connects to the PC (laptop) for real-time display and recording of temperatures, Figure 18.

Figure 17 - T-type thermocouple for cryogenics, fully equipped with plug

Figure 18 - Termometru digital Mastech MS6514

8.4 Cooling equipment The temperatures and experimental protocols will be obtained and controlled with three types of equipment: *a cooling bath with mechanical compression conveying a liquid thermal agent*, consisting of a mixture of water and glycol, concentration 50%, *a conventional* industrial freezer using a mechanical compression cooling plant and a cryogenic deep-freeze freezer for very low temperatures, using liquid nitrogen as a cooling medium.

A Lauda cooling bath model RE 1225 S, manufactured in Germany by LAUDA DR. R. WOBSER GMBH & CO. KG. In Figure 19 We have prepared a representative figure.

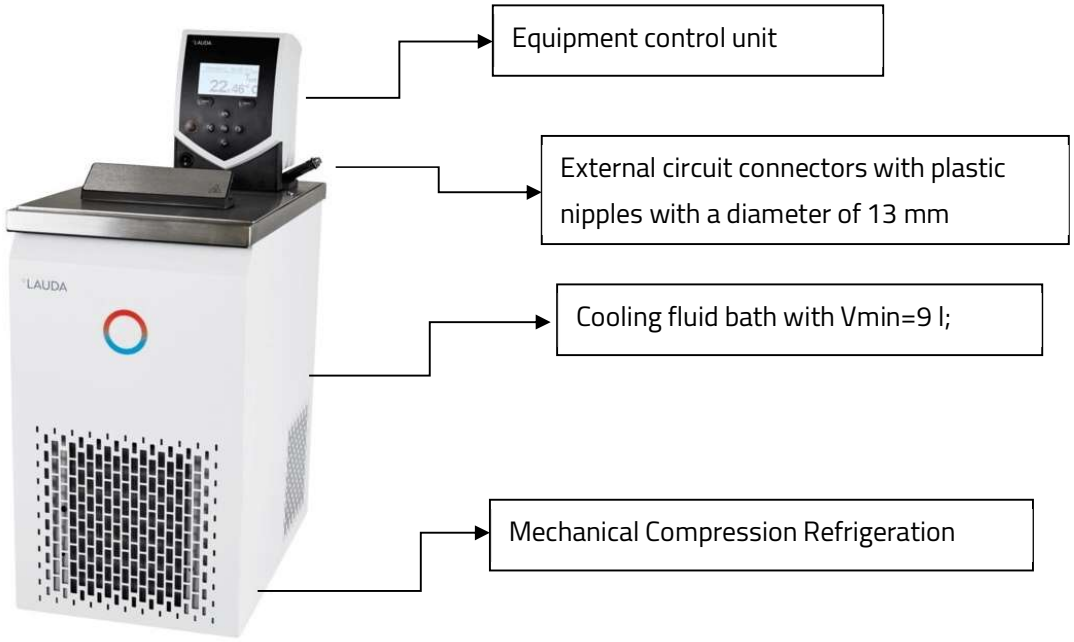

Figure 19 - Lauda 1225 S control and cooling unit

The second cooling equipment that was used in the experiments is an industrial freezer from Vestfrost model VT407. The VT low-temperature freezer creates the possibility of maintaining temperatures between -40°C and -60°C by being served by a very economical mechanical compression refrigeration system (7,077 kWh per day).

Figure 20- Vestfrost V407 industrial freezer

A cryogenic freezer used in laboratories, with well-defined performance and temperatures in the range of 40°C and -180°C. For operation in deep cold temperatures, the cooler is supplied with liquid nitrogen from an external tank with a maximum operating pressure of 15 MPa. Figure 21.

Figure 21 - Congelator criogenic tip Planner Kryo 360 3.3 MRV

8.5 Microscop digital, For visual studies, a *microscop digital* high-performance with a high resolution and a focal length of at least 50mm, Figure 22.

Figure 22 - Microscop digital Easyover

8.6 Viewing Device.

A huge pressure that the transparent elements must withstand must be taken into account, namely 100 MPa at a temperature of -10°C or around 200 MPa at a temperature of -20°C. The main purpose being the visual study inside the isochoric reactor before but especially after the nucleation is triggered, I turned to compatible materials that combined could use this objective. After analyzing several materials, we came to the conclusion that the most suitable would be a hard aluminum alloy code 7075-T6 used in the aeronautical industry, being recognized for its hardness, low weight and high thermal conductivity.

Once these aspects were defined, several design iterations followed, which finally led to the final version of the model. The significant differences and improvements that helped me achieve the goal were: choosing a material with a thermal conductivity coefficient higher than 3.5 times that of sapphire, complete assembly. I have chosen each component part carefully, paying attention to the manufacturer and supplier to ensure that they will be able to fully meet the performance requirements necessary for the project. Therefore, the 7075-T6 aluminum block was purchased from *SC MRG STAINLESS GROUP SRL,* The synthetic sapphire glass has been made to order according to exact dimensions and with precision at the *Precision Sapphire Technologies, Ltd* Lithuania, o-rings from *Hydraulic* Brașov-Săcele, and the couplings and screws from specialized

local stores. The result obtained was commensurate Expected. In Figure 23 The project with the components of the device is presented.

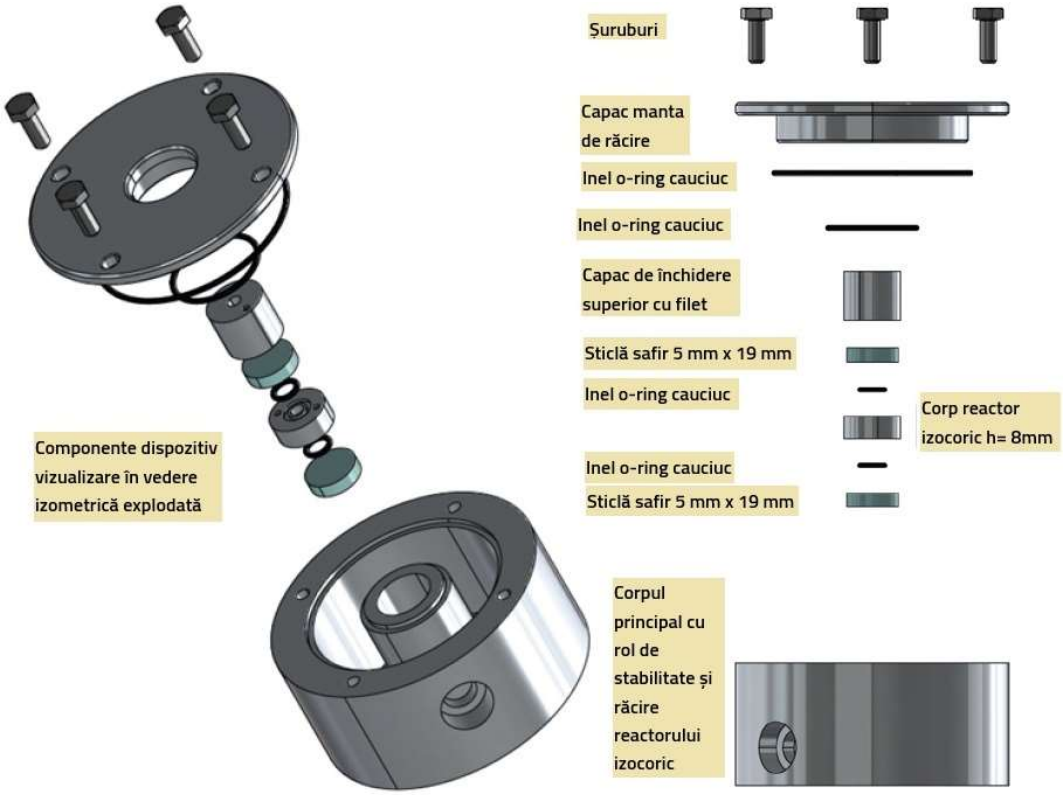

Figure 23 - Isochoric viewfinder, exploded component view rendering

Figure 24 - Isochoric visualization device – the real model, with its functional components disassembled

For clarity and a better understanding of the whole, we still have some renderings with sections in Figure 25 and Figure 26 where you can see how the components look when they are merged. The isochoric chamber is practically hermetically sealed with two transparent sapphire glass caps. O-rings resistant to temperatures down to -25°C were used to seal them, but replaced at each experiment, for safety, because the pressure to which they are exposed destroys them.

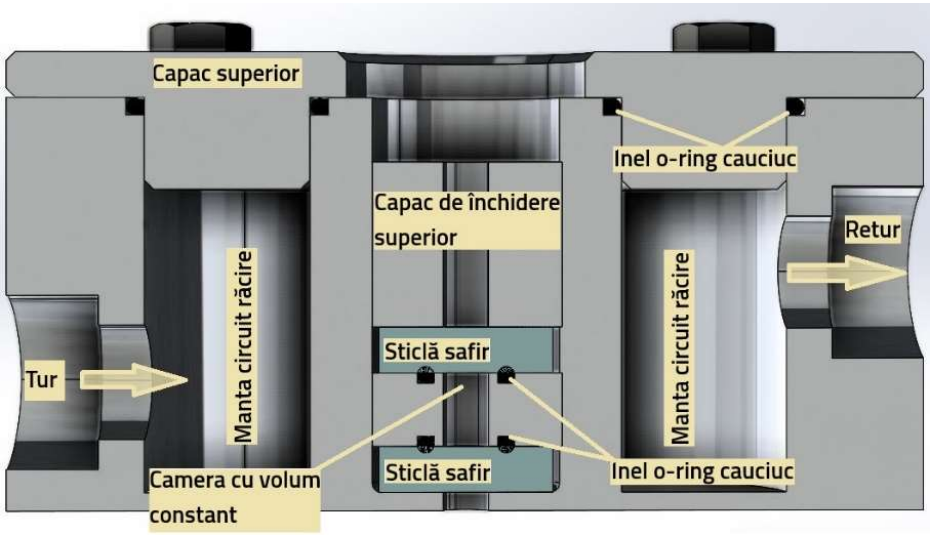

Figure 25 - Isochoric visualization device section

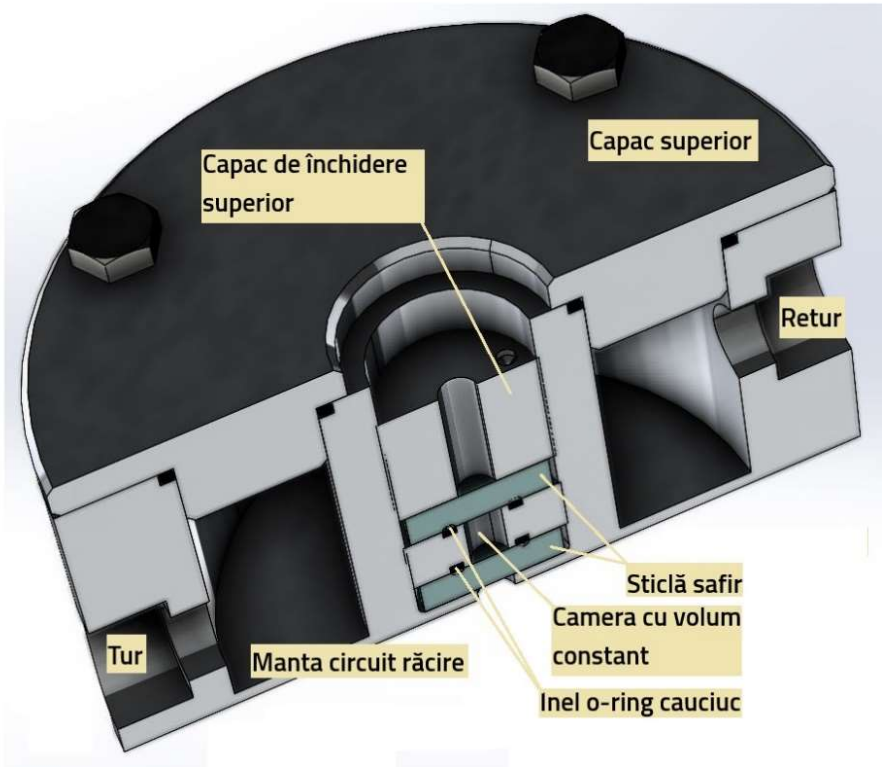

Figure 26 - Isometric section isochoric visualization device

9. CHAPTER 9: Results of experimental studies

9.1 Comparative study between two techniques for stabilizing the state of water supercooling

9.1.1 Introduction

I will present in this subchapter an experimental study on the kinetics of ice nucleation comparing two techniques for presenting the supercooling state: the first, the isobaric one, separating the media with a layer of oil and the second, supercooling in an isochore medium. A series of experiments in which we maintained a constant cooling rate, compare the apparent nucleation temperatures of supercooled pure water using the two techniques, with conventional isobaric supercooling, demonstrating that both methods significantly improve the stability of the supercooling state of the system compared to supercooling in contact with atmospheric air. While the average nucleation temperatures of the two methods are statistically comparable, isochoric supercooling exhibits about half the variability of oil-sealed isobic supercooling, which may have important implications for the design of supercooling-based biopreservation protocols where stability and reproducibility are critical. The practical study brings to the fore an evaluation of the effective nucleation temperature of the ice, for pure water, under conditions: isobaric but having a separation of contact with the atmospheric air by applying an oil film, isochores and conventional in direct contact with the open air. The cooling rate remained constant throughout the experiments and the variability of the ice nucleation temperature was considered as a measure of the relative stability between the techniques compared. We used MS-1 type isochoric reactors and digital pressure transducers, designed specifically for these applications.

9.1.2 Experimental Protocol

The three thermodynamic conditions examined were applied as follows:

1) for isochoric conditions, the reactor has been filled with distilled water and completely sealed, carefully to avoid the introduction of bulk air bubbles (which can damage isochoric conditions due to their high compressibility);

2) for isobaric oil sealing conditions, an identical chamber was filled with distilled water, but instead of the pressure transducer, we covered the water with a layer of about 2 mm high of partially synthetic oil, thus maintaining a constant atmospheric pressure, but eliminating the air-water interface;

3) For conventional isobaric conditions in atmospheric air, we filled the third identical chamber, leaving the topmost liquid surface, unsealed and exposed to the environment.

Figure 27 E and D, show typical temperature and pressure paths observed in experiments, with the arrows marking the precise onset of the nucleation phase. For consistency, after verifying the overlap in time between the onset of nucleation, based on the sudden temperature fluctuation but

also on the sudden effect of pressure, we used only the temperature data from the thermocouples mounted on the outer surfaces on the three chambers, for comparison and subsequent analysis by means of a single common denominator: temperature. Figure 27 Is.

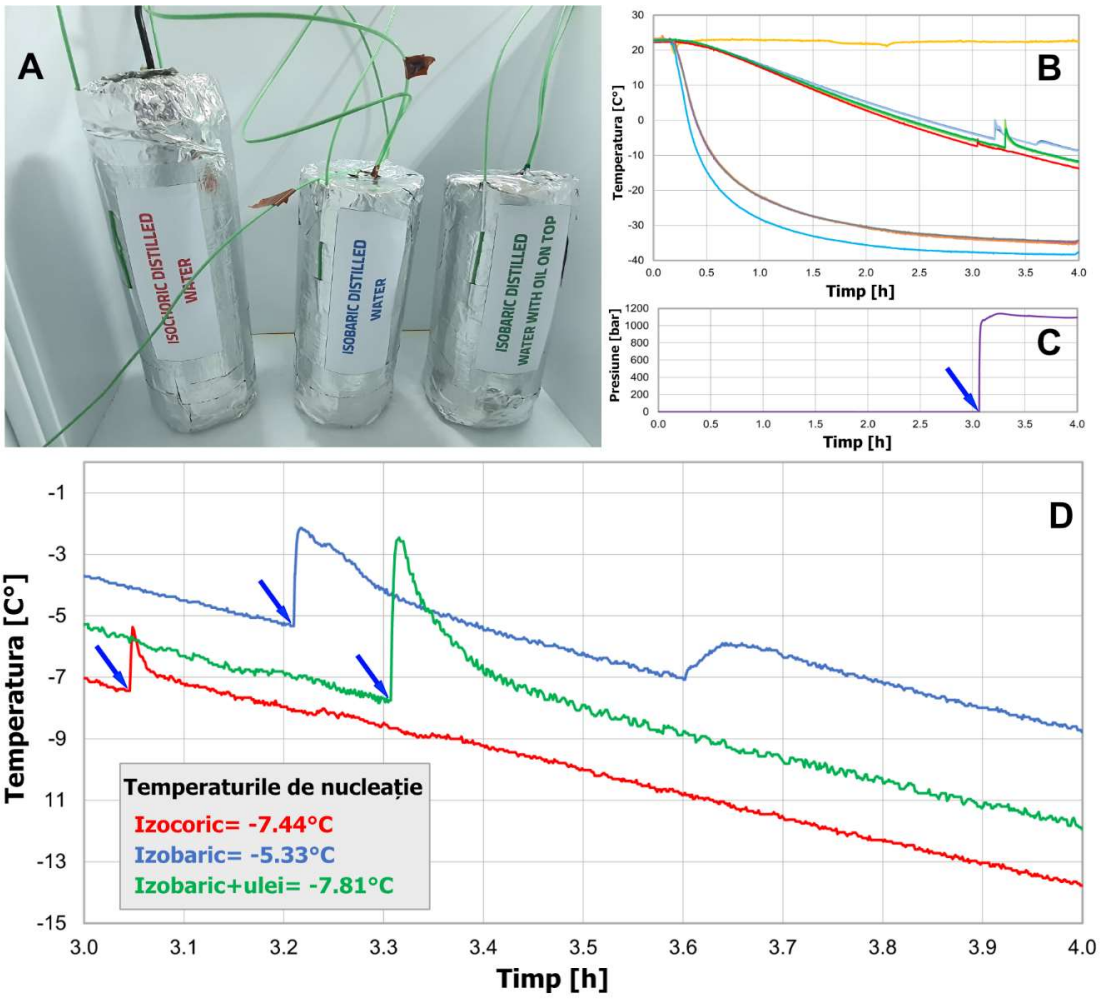

Figure 27 - A. The 3 reactors inside the freezer; B. Typical graph for all recorded temperatures; C. Graph of pressures, with the arrow indicating nucleation; D. Graph of temperatures recorded on the outer surface of the reactors.

9.1.3 Results

The results presented in Figure 27 shows the nucleation temperature measured in each of the three systems in 12 experiments. The statistical analysis of these data to compare the effects of thermodynamic conditions on nuclear temperature was performed by ANOVA, unidirectional, with Bonferroni's method used for the multiple comparison test, and the cassette diagrams are presented Figure 28. Statistical analysis demonstrates that both isobaric and oil-sealed isochoric supercooling suppress the likelihood of kinetic nucleation of ice compared to conventional isobaric supercooling in the open air ($p < 10^{-5}$ for each) and that these two techniques provide a statistically similar improvement for the stability of the subcooling phase (e.g., suppression of the observed nucleation temperature) ($p = 0.67$). Importantly, however, there are notable differences in the consistency with which these techniques produce a stabilization for the subcooling phase, as demonstrated by the dynamics of the data. While the arithmetic means of the nucleation temperatures produced by oil-sealed isobaric supercooling and isochore are statistically equivalent, the standard deviation of these nucleation temperatures is almost twice as large under isobaric oil-sealed conditions (standard deviation = 1.66 °C) than under isochoric conditions (standard deviation = 0.90 °C), indicating greater stability of kinetic supercooling under isochoric conditions, except under isobaric oil sealing conditions.

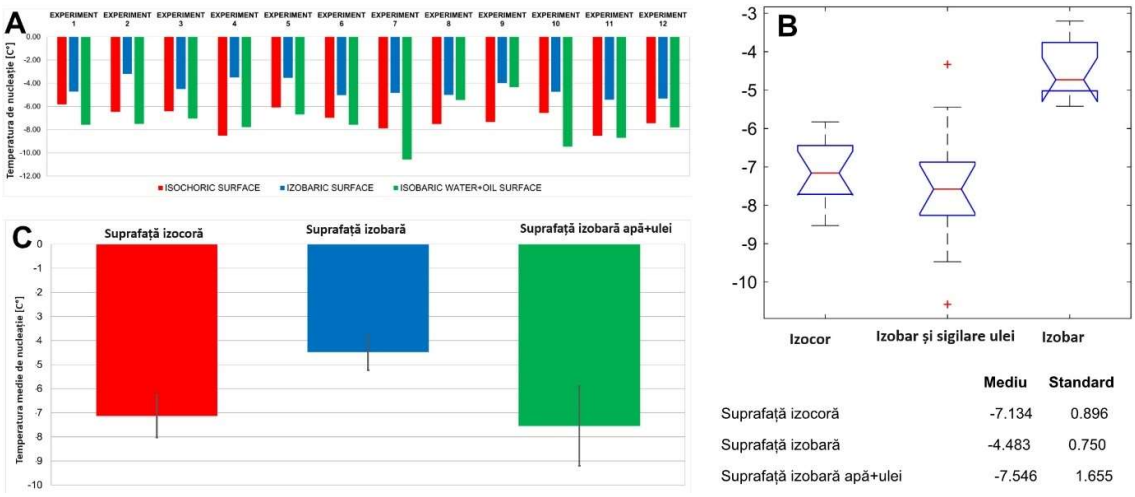

Figure 28 – A. Nucleation temperature measured in 12 replicates for each of the three systems; B. Diagrams for isochore, oil-sealed isobaric and conventional isobaric supercooling state in contact with atmospheric air; C. Diagrams for the average nucleation temperatures in the three systems

These results confirm, in a dynamic context, the previous findings of isoporic supercooling in steady state and isobaric oil sealing studies [12], [25] . As found in both previous studies, both techniques improve supercooling stability compared to conventional supercooling; however, consistent with previous findings that isochoric conditions provide superior stability in the face of various mechanical disturbances, our data here demonstrate that they also confer a higher degree of

stability against kinetic nucleation during the cooling process, providing more predictable behavior and greater certainty of avoiding nucleation at lower supercooling temperatures.

In conclusion, we observe that this study represents a completion in the understanding of the properties related to the relative stability of the water supercooling state and the nucleation triggers, using the isochoric or oil-sealed isobaric method. Future studies should examine the actual nucleation temperatures and variability in systems with increasing volume, as well as the induction times of steady-state nucleation as a function of temperature, in order to complete the overview and clarify the practical limits of the stability of supercooled liquids relative to nucleation.

9.2 Study of the isochoral freezing behavior of a water-based substance used in the medical field, especially for organ preservation (Custodiol)

9.2.1 Introduce

Among the most interesting applications that are based on the notions investigated in this paper are the conservation of biological matter in a controlled environment with constant volume (isocor) at negative temperatures, reaching the metastable state of subcooling. A notorious cryopreservation substance is Custodiol which is indicated for the infusion and washing of organs: kidneys, liver, pancreas and heart of the donor. So far, there are no representative and relevant temperature-pressure data on a cryopreservation protocol below 0°C for Custodiol. In the experimental procedures, we used an isochore reactor, fully equipped to simultaneously measure both temperature and pressure inside the constant volume chamber.

9.2.2 Experimental Protocol

For the first type of procedures we followed the following program: the temperature of the cooling bath was initially set at 0°C. The studied temperature thresholds start from 0 °C and decrease in 5 °C increments to -25 °C. That is, we will have the thresholds of -5°C, -10°C, -15°C, -20°C and -25°C. The time it took for the system to reach each temperature threshold was between 20 and 90 minutes, with the longest time being from -20 °C to -25 °C. The period allocated for maintaining the thermal equilibrium at each threshold The reference temperature was 15 minutes except for the end point at -25°C where the hold was 50 minutes. After introducing the microreactor into the cooling bath, a thermodynamic equilibrium followed at 0 °C for 15 minutes and then the temperature modification program was started according to the procedure described above, until the value of -25 °C was reached. After 50 minutes of equilibrium at the last reference temperature point, we went through the melting process in the same temperature thresholds that we had at the freezing phase. We thus got back to 0 °C by keeping each temperature point at thermodynamic equilibrium for a time of 15 minutes. It is worth mentioning that on the melting (heating) zone, the temperature thresholds are reached faster, the average time being about 5 minutes for each threshold, to which are added the 15 minutes of capping at thermodynamic

equilibrium of the set point. Thus, the linearity in the heating process will be graphically observed, in antithesis to the variability in the cooling process. A representation of the temperature protocol is presented in Figure 29. Blue is the temperature set in the cooling bath controller program, and orange is the actual temperature in the cooling bath. We notice that they overlap, which means very precise temperature control. Cooling lasts over 3 hours and 30 minutes while melting occurs in less than 1 hour and 30 minutes.

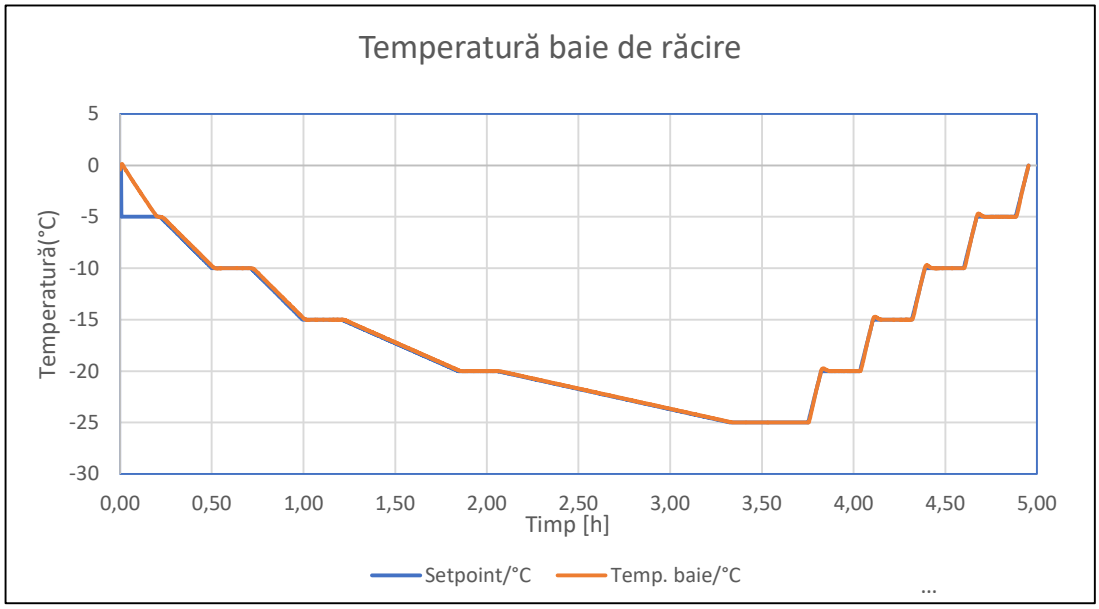

Figure 29 - The temperature chart of the cooling bath on the cooling phase from 0°C to -25°C and on the heating phase from -25°C back to 0°C as a function of time.

For the second set of procedures, the cryogenic freezer was used, which uses liquid nitrogen as a coolant. The nucleation temperature in the isochore chamber was determined by correlating the temperature measured on the outer surface of the chamber with the pressure detected by the attached pressure transducer.

9.2.3 Results and discussions part 1 – temperature-pressure correlation

Each of the 8 experiment sessions we considered, took place over a duration of 6 hours, in which the temperature and pressure parameters were constantly monitored and recorded through the equipment described above. Each session of experiments had different results in terms of the temperature-pressure zone in which the cryopreservative Custodiol was in a state of subcooling and the point temperature in which nucleation occurred. The pressure in the isochore chamber had a hydrostatic behavior, and any changes in pressure propagated with the speed of sound. These pressure changes were directly related to the freezing of water inside the isochoric chamber but also induced by the same phenomenon. Given the interdependence of pressure and temperature in an isochore system, monitoring pressure changes served as an effective indicator of the

thermodynamic state inside. Specifically, when the pressure sensor stopped detecting any subsequent pressure fluctuations, it meant that thermodynamic equilibrium had been reached within the system. Usually, the time required for the system to reach this state of thermodynamic equilibrium falls within the range of 15-60 min. The data collected by these procedures are presented below and arranged in a series of thermodynamic profile figures, which include the data obtained from 2 experimental sessions out of the 8 carried out. They display the pressure as a function of time. The temperature was changed gradually, and the constant temperature values used in this set of experiments are listed on the horizontal lines in the figures.

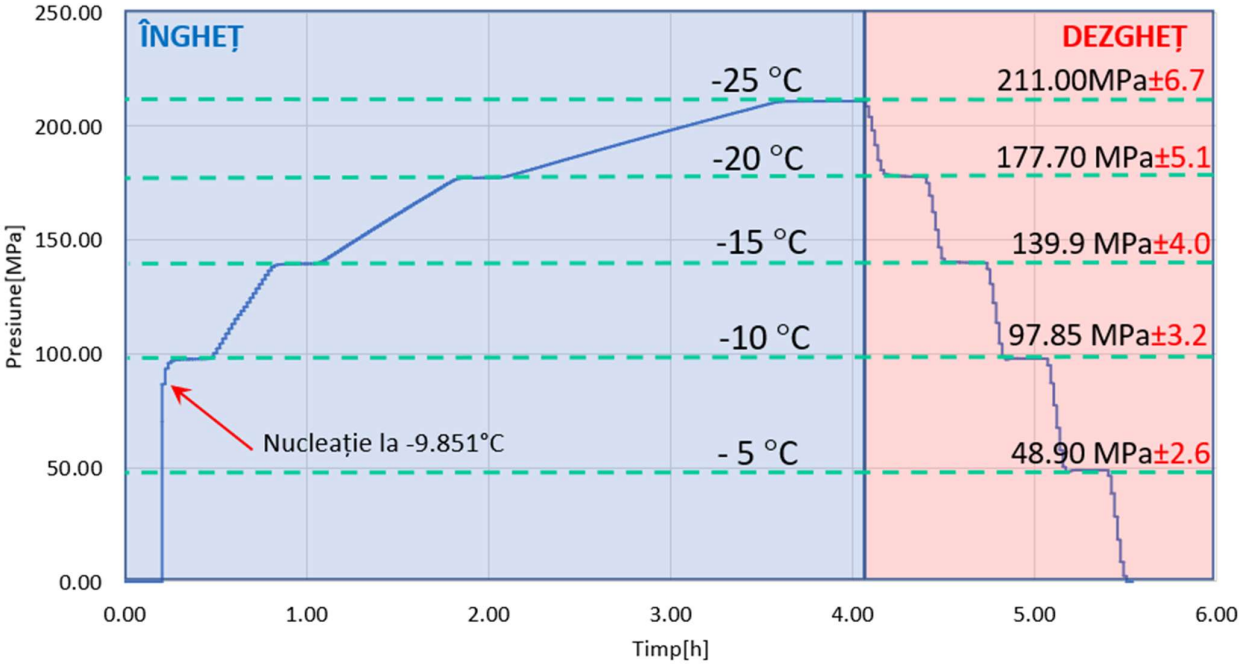

Figure 30 - Thermodynamic profile (temperature-pressure), under constant volume conditions (isocor) for Custodiol with the nucleation temperature at the threshold of -9.851°C (Experiment 4)

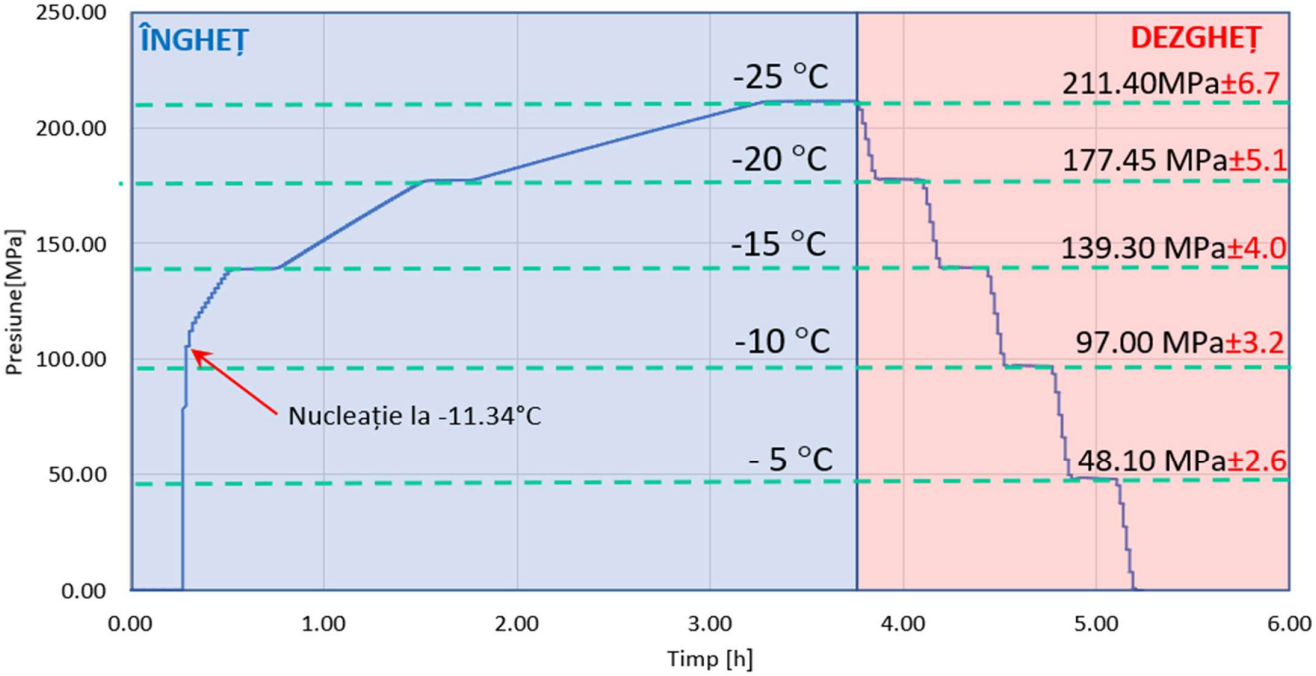

Figure 31 - Thermodynamic profile (temperature-pressure), under constant volume conditions (isocor) for Custodiol with nucleation temperature at the threshold of – 11,734°C (Experiment 5)

By following the data presented graphically and tabulally, they can be interpreted in multiple ways. Relevant is that we have isochore supercooling in each set of experiments. Another interesting observation is that the same pressure values were obtained at the specified constant temperatures both during cooling and during heating to those reference temperatures, and there was no hysteresis. For the temperature of -5°C during frost in all experiments there are no data. This is because the supercooled system and freezing by random nucleation has always occurred only at a temperature lower than -5 °C.

9.2.4 Results and discussions part 2 – heterogeneous nucleation temperature

The experimental setup was made to directly touch and then stabilize at a temperature of -20°C through the cryogenic freezer, starting from room temperature. The successful achievement of thermodynamic equilibrium is clearly visible in the graph in Figure 32. The time interval was approximately between the 82nd and 135th minute. The temperature that defines this graph corresponds to the temperature in the cryogenic freezer chamber, which is measured by means of a thermocouple fixed on the outside of the isochoric reactor. This temperature is not the same as that of the liquid inside the isochoric reactor. Also in the same graph from Figure 32 Both temperatures and pressures measured during cooling are presented. The moment when the pressure begins to increase indicates the onset of ice nucleation. We consider the heterogeneous isochoric nucleation temperature to be the temperature recorded right now.

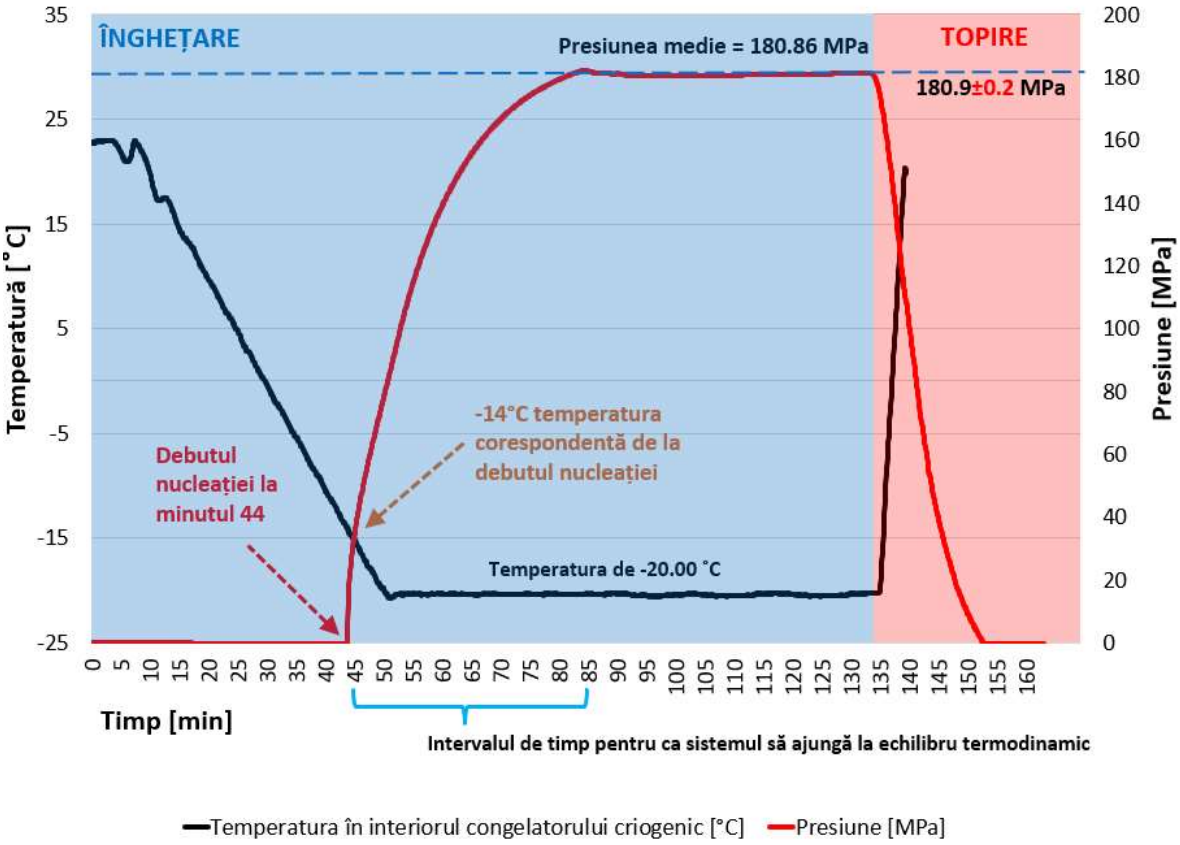

Figure 32 - Values of temperatures and pressures during cooling to identify the nucleation temperature

The isocore chambers were equipped with thermocouples on the outer surface in the same location for each. The onset of nucleation is marked by the recalescence (a sudden increase in temperature) that accompanies crystallization in supercooled liquids, which has been monitored by means of these thermocouples for all reactors.

Figure 3333. In addition, because in the case of the isochoric chamber the frost is partial, only part of the interior content turns into ice, causing a much less significant recalescence, the detection of nucleation is established by following the pressures that experience a sudden increase.

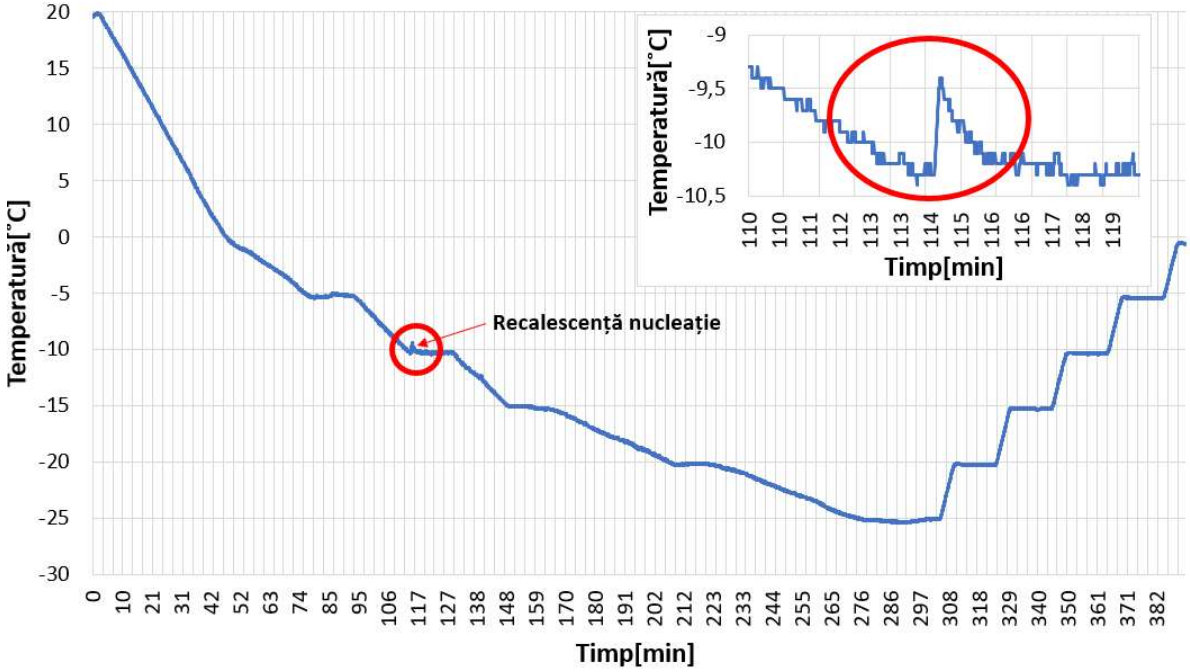

Figure 33 – Surface temperature of isochoric reactors for identification of nucleation temperature in distilled water experiments.

The statistical analysis of the data for the comparison of the heterogeneous nucleation temperature for Custodiol and distilled water, was performed by the ANOVA method, in one direction, using Tukey's test for multiple comparisons. We have thus generated a box diagram that can be viewed in Figure 34. Statistical analysis demonstrates that the nucleation temperature for Custodiol and distilled water, in the isochore medium are almost the same.

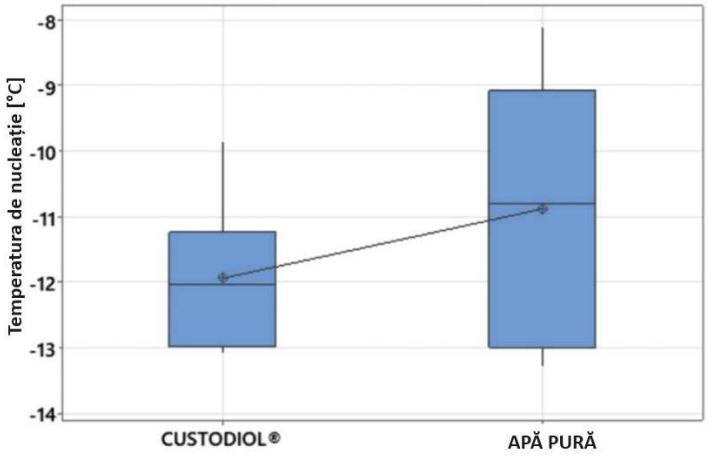

Figure 34 - Box diagrams for the nucleation temperature of the Custodiol solution versus the nucleation temperature of pure water under isochoric conditions.

The main purpose of this study was to correlate pressure and temperature for a commercial solution used in the medical field for organ preservation.

9.3 Visual study of the phenomenon of nucleation in isochoric regime

9.3.1 Introduce

Once all the parameterization tests were completed, we started a series of trial experiments, where the main goal was to objectively observe the operation of the system, collect the first images, adjust the focus and optimize the digital microscope. The actual transparent diameter through which the frames are taken is 5 mm. The process of testing, preparing and parameterizing the system was not a simple one, but it prepared the ground for the actual experiments to be carried out in the most optimal conditions.

9.3.2 Experiment protocol

1) Placing the lower sapphire glass in its position.

2) The constant volume reactor (isochore) is screwed into the internal channel of the body, being sealed by means of the o-ring that presses the lower lens.

3) After the filling operation has been carried out correctly and carefully, we carefully place the upper sapphire glass, which will also be sealed by means of the o-ring.

4) The whole assembly is stiffened and hermetically sealed, being prepared for cooling.

5) The acrylic plastic condensation protection screens are properly positioned and fixed with adhesive tape. To avoid condensation, dry air from the spray was introduced into the space between them and the sapphire.

The temperature of the isochore reactor is controlled by a continuous flow of thermal agent through the cooling jacket. For accuracy, the inlet and outlet temperatures of the coolant are continuously measured and recorded using the two T-type thermocouples.

The experiments were carried out between two temperature thresholds: starting at 5 °C and going down to a minimum of -13 °C. We have also defined 3 reference temperatures for which we have established to maintain the thermodynamic equilibrium: – 6 °C, – 9 °C and – 13 °C. The recorded cooling rate averaged 18 °C/h. We know from previous studies that water in isochore spaces freezes randomly in the temperature range of -7 °C to -10 °C. This fact has also been demonstrated visually in experiments. Once nucleation occurs, we will again maintain an equilibrium temperature threshold at -9°C for the visualization of the equilibrium state. It then continues cooling to the final reference point. A few minutes after reaching thermodynamic equilibrium, a positive temperature of +5 °C is set to visualize the melting phase. Melting is usually visible after the thermocouples sense the temperature of + 2 °C of the heating agent. [26], [27]

9.3.3 Results, tracking the dynamics of the ice core, in a finite and constant volume (isocor), freezing:

At the zero point of each experiment we had in the foreground the image of liquid water, without air bubbles, practically observing a homogeneous, clear and transparent environment. Around the temperature of -8.4 °C, the system experiences a sudden, rapid and very brutal onset of homogeneous nucleation from the liquid aggregation state to the solid aggregation phase. The first five seconds after nucleation are shown in Figure 35 and are marked by very rapid changes. The microscope camera has the ability to record up to 30 frames per second. It is important to note that the instance Time=0 s refers to the moment T0' just before the nucleation and not to the moment T0 when the experiment began. The radial geometry of the reactor walls is replicated by ice crystals, as can be seen in the images. The ice has a dendritic morphology and it is observed that the first 5 seconds after the onset of nucleation resemble those in an isobaric environment [27] . The walls of the reactor behaved as I predicted, they were basically triggers of nucleation. This can be seen from the 0.05-second frame that shows on the left side some fine formations of ice crystals as a result of the nucleation trigger.

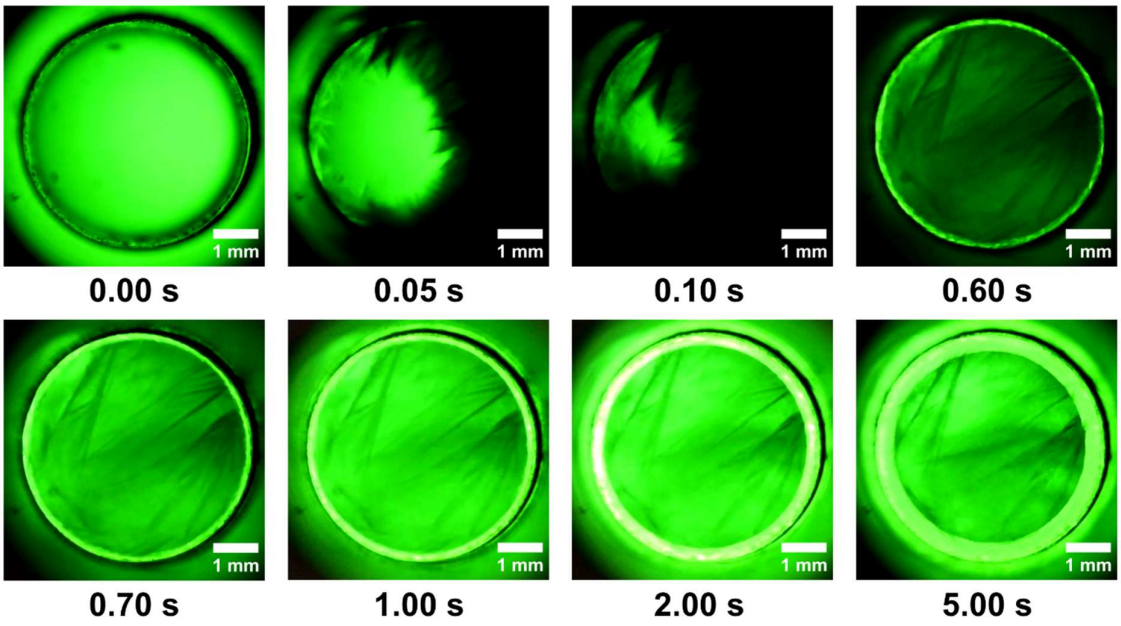

Figure 35 - The first 5 seconds after the onset of nucleation in the isochore. Note* - the static black spots in the first left image are anomalies on the microscope lens plate [29] .

Already after 5 seconds, the tendency of a liquid nucleus to concentrate from the outside to the inside is observed. Ih ice formations expand at a significantly slower rate after the first ten seconds after nucleation. This slowdown was caused by an increase in internal pressure approaching 90 MPa. In turn, the container whose internal volume remains constant, will apply equal and opposite pressure to the mixture of water and ice. We now refer to this pressurization of the system as the

"isochoric growth penalty", which represents the energy cost incurred by the solid phase to increase in a system of absolute and specific limited volume. In [28] Figure 36, these phenomena can be observed. After the first 10 seconds of the onset, the dynamics slow down significantly by increasing the internal pressure, the total crystallization process is restricted.

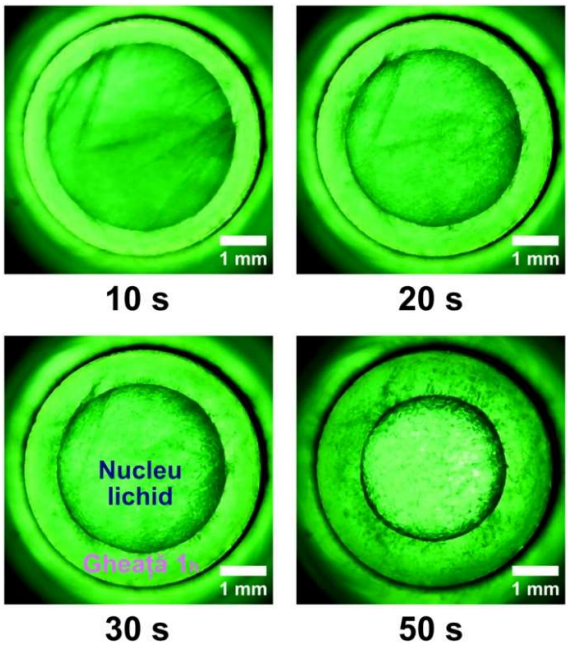

Figure 36 – The early stages of ice crystal development, immediately after nucleation. You can see the first 50 seconds [29]

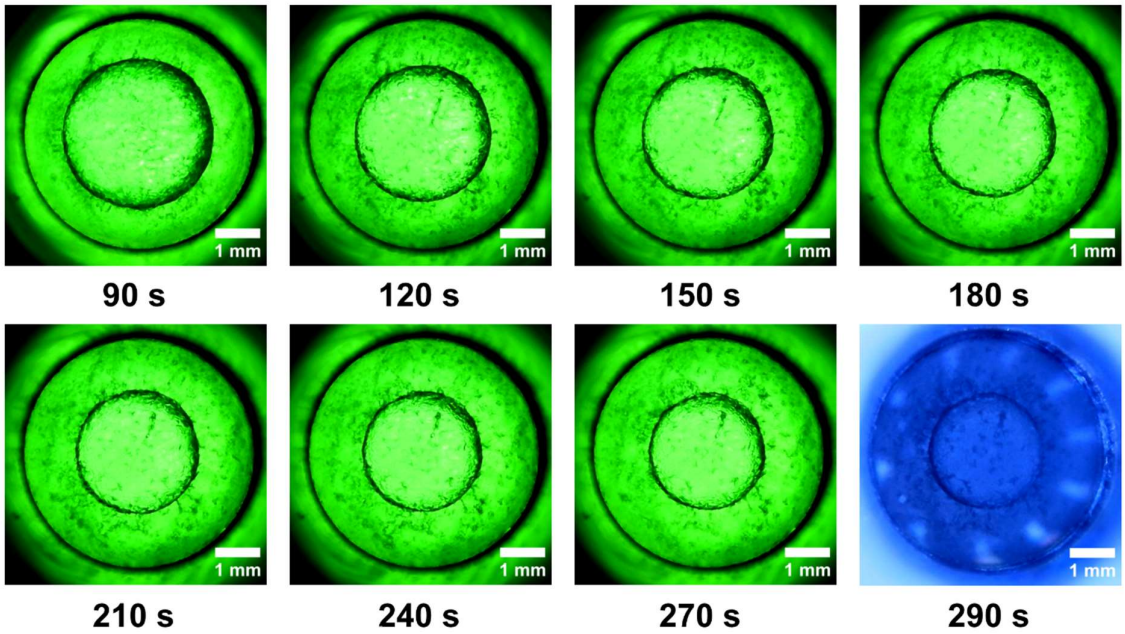

Figure 37 - Almost 5 minutes after nucleation. The last picture is captured with the upper light, blue tint because there were no color filters present. White dots are the reflections of LEDs that illuminate. [29]

9.3.4 Results, tracking the dynamics of the ice core in a finite volume and constant (isocor) melting:

After the steady state was confirmed at -9 °C, we completed the cooling process. The temperature has been set at 5 °C positive temperature, with an average heating rate of 60 °C/h. The first signs of melting are observed on the outside of the ice sheet (the dark edges of the 38).

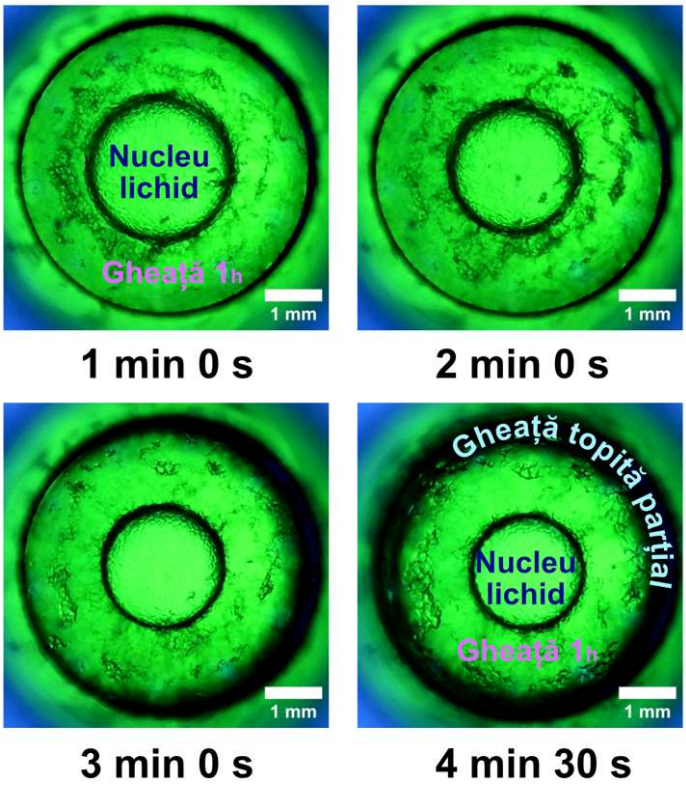

Figure 38 - The first 4 and a half minutes after the start of the melting phase [29] .

It is observed how the warm wall of the reactor quickly melts the ice, and the liquid form of the water begins to increase significantly at the expense of the thinner and thinner ice layer. In Figure 39, 8 image captures with an equal step of 15 seconds are shown, where the thawing is visualized becoming more and more accelerated. The ice now floats in the liquid that surrounds it. In the last frame of Figure 39 You can see how the ice actually disappears when it comes into direct contact with the hot wall of the reactor.

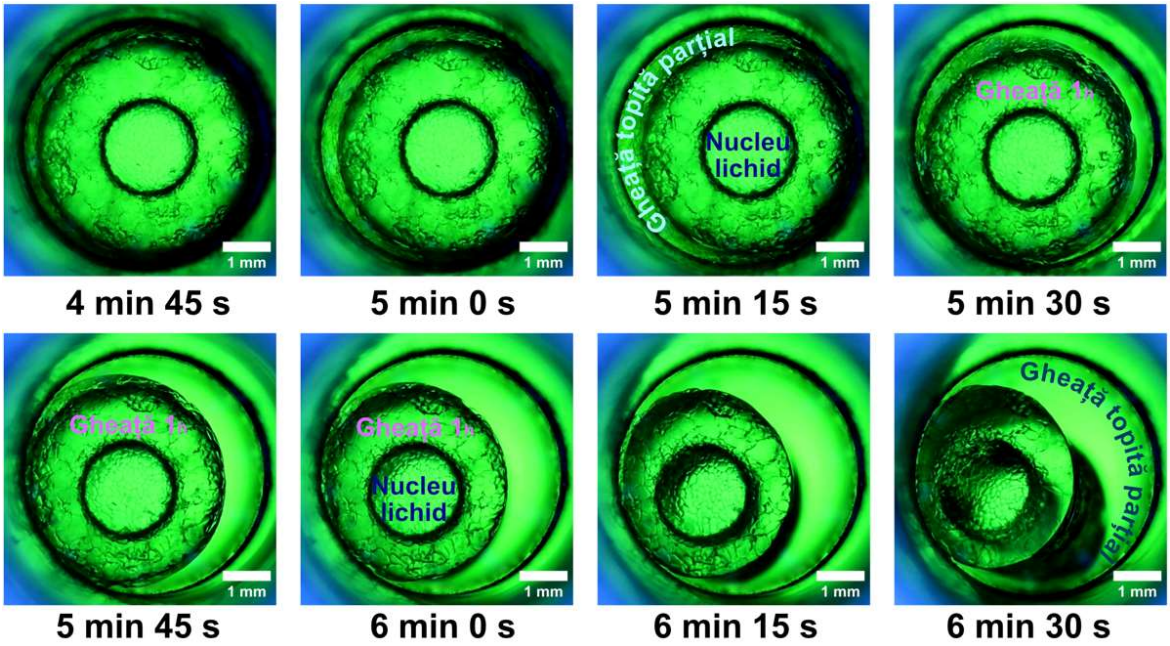

Figure 39 - Defrosting process in progress. Time is quantified from the moment the melting process began. 15-second step between frames [29] .

The thawing phase continues to accelerate, which is why in Figure 40 I exemplified a series of images captured with a 10-second step. We notice how a hole has remained well defined in the center of the ice cylinder. This is due to the fluid core, captured inside, by the ice that has formed all around. The ice disappears completely 10 minutes and 23 seconds after the start of the warm-up stage. The system arrives in the same visual state as it was at the beginning of the experiment, before freezing. The image is clean, transparent, without air bubbles. Which denotes the fact that the tightness was correct, so one can affirm the success of a complete cycle of experiment, freezing and then thawing, in an isochore system.

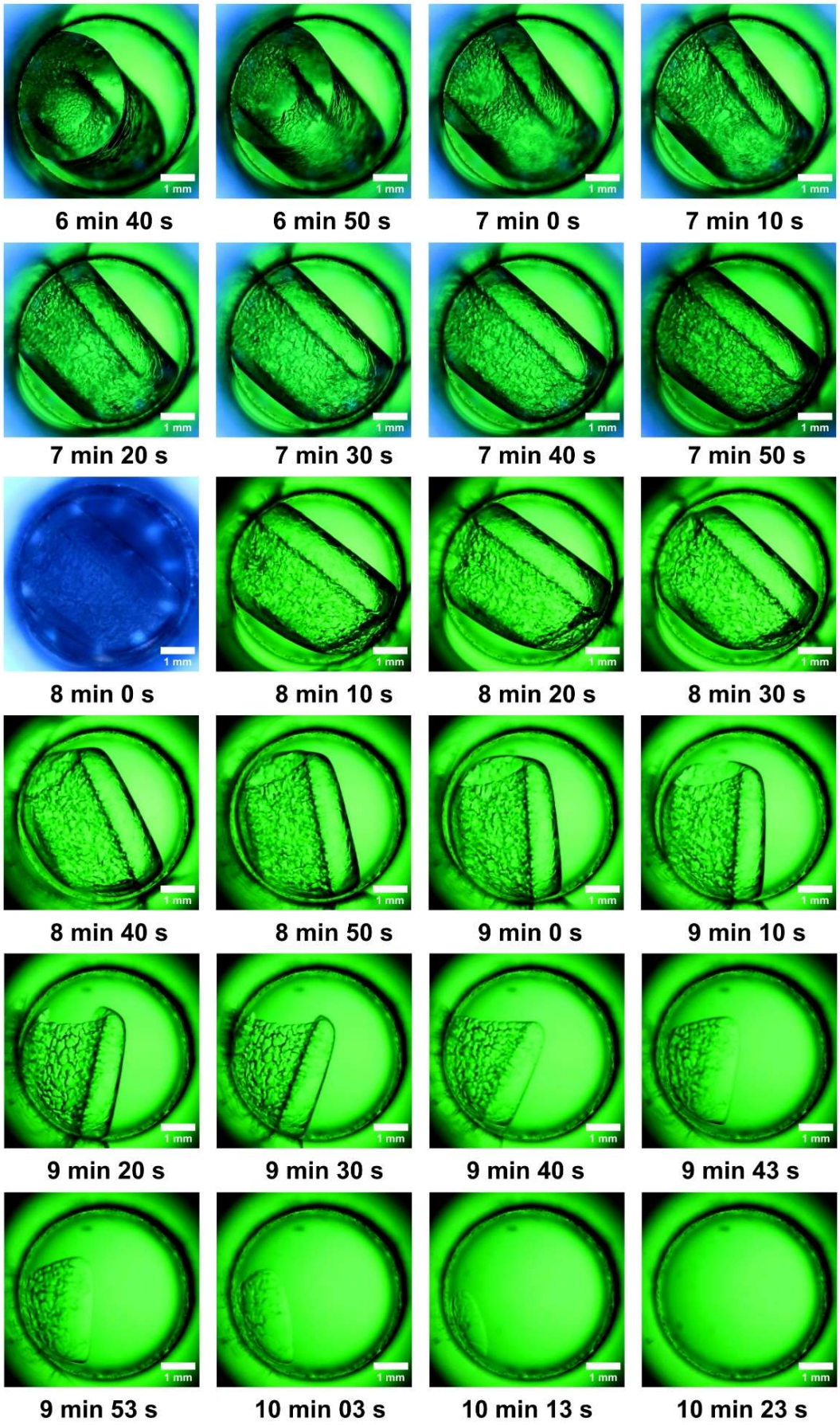
1 mm
6 min 40 s
6 min 50 s
7 min 0 s
7 min 10 s
7 min 20 s
7 min 30 s
7 min 40 s
7 min 50 s
8 min 0 s
8 min 10 s
8 min 20 s
8 min 30 s
8 min 40 s
8 min 50 s
9 min 0 s
9 min 10 s
9 min 20 s
9 min 30 s
9 min 40 s
9 min 43 s
9 min 53 s
10 min 03 s
10 min 13 s
10 min 23 s

Figure 40 - Defrosting process in the final stage. The entire liquid-ice mixture in the reactor is returned to its original state. 10-second step for the first 19 frames, 3-second step for image number 20, then 10-second step until the end [29]

9.3.5 Results. Tracking the dynamics of the ice core in a finite and constant volume (isochore), prolonged freezing after the triggering of nucleation:

Further I will present a case in which the cooling bath continued to pump heat at a set temperature of -13°C, the freezing phenomenon can be visualized in Figure 41. The formation of a liquid core that resists the freezing phase is also well identified here. The ice increases in volume as the temperature drops. The diameter of the liquid core decreases and acquires an uneven shape with protrusions in the ice area. After 19 minutes and 20 seconds after nucleation, the system is thermodynamically balanced at a temperature of -11.7 °C, as confirmed by the equalization of the inlet and outlet temperature of the coolant.

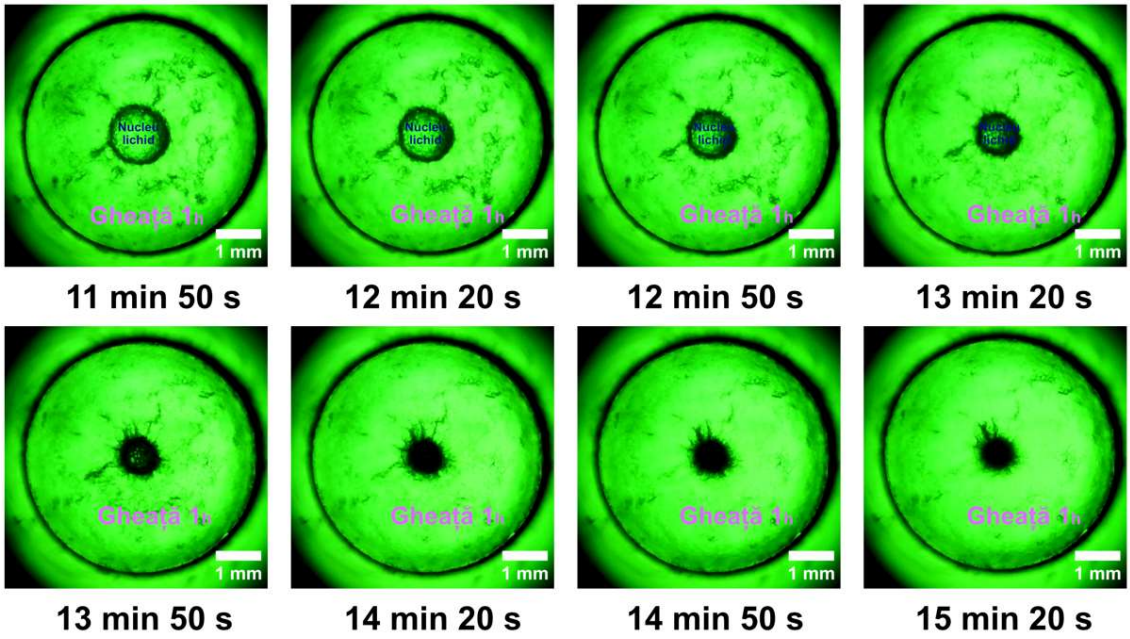

Figure 41 - The phenomenon of nucleation and crystallization of ice until reaching the thermodynamic equilibrium temperature measured at – 11.7°C (– 13°C temperature actually required on the cooling bath) [29]

9.3.6 Results. Tracking the dynamics of the ice core in a finite and constant volume (isocor), conclusions

In terms of location, the ice originates from the walls of the reactor, which serve as a starting site for nucleation. The internal pressure of the system increases as the ice spreads, decreasing the rate of propagation and the amount of water turned into ice. As a result, a liquid core is concentrated inside and the ice stops forming. These details are essential because they provide clear indications

of where the biological material should be safely stored for cryopreservation, so that the ice crystals do not damage the tissue.

Melting, the opposite phenomenon, was equally fascinating and unique. It was visualized immediately after the aggregation phase, Figure 37. At first, the dynamics are relatively slow due to thermal inertia. Melting gives us some spectacular images of liquid on the edges of the reactor, then ice, and then liquid inside the ice cylinder again. As the heat agent flows through the reactor mantle, the melting ice inside the reactor begins to rotate and float in that direction, producing images from multiple angles, Figure 40. The water eventually becomes as clear as it was at the beginning of the experiment, without any evidence of the existence of the ice crystal. Since an entire freeze-thaw cycle was performed inside the isochore reactor, the experiment is considered to have been successfully completed.

10. CHAPTER 10: Final Discussions and Conclusions

Water plays an essential role in nucleation processes, both in the context of biotechnology and bioengineering, as well as in atmospheric phenomena. In biotechnology, water is a universal solvent that facilitates the dissolution and transport of substances necessary for protein crystallization and the formation of biomaterials. In bioengineering, water is crucial for maintaining the moist environments necessary for the growth and development of lab-grown tissues.

In atmospheric phenomena, water is fundamental for the formation of clouds and precipitation. The nucleation of water droplets and ice crystals is an essential process in the hydrological cycle, influencing weather and climate patterns. Water's ability to form hydrogen bonds contributes to the structure and stability of droplets and crystals, having a direct impact on cloud formation and dynamics.

Research on isochoral nucleation provides valuable insights for the control and manipulation of phase transitions in complex systems. For the future, it is recommended to expand the studies to include the effects of impurities and external fields on nucleation. Future studies should also focus on developing more accurate predictive models and experimental techniques that allow real-time, nanoscale nucleation observation.

The study and understanding of the behavior of water or other aqueous substances at a constantly restricted volume can provide the essential answers for the development of new technologies for the conservation of organic matter. So far, studies have demonstrated the efficiency of preserving some vegetables and fruits [30] [31] [32] [33] [34] [35] [36] [37] , single or multi-cellular microorganisms, animal or human tissues, using isochore cooling and freezing. In order for such applications to be possible, it was necessary to carry out studies that would reveal crucial and relevant information in the description of the thermodynamic processes that underpin conservation protocols. [38] [39] [40] [41] [42] [43] [44] [45] [46]

The comparative study carried out between the methods of increasing the metastable state of water supercooling revealed that using only containers of finite and constant volume, the nucleation temperature barrier was exceeded above the values that would have been obtained by adding cryopreservation substances.

We brought up the topic of applicability in the medical field and this was the motivation to choose a substance frequently used in transplant medicine, for which there are no thermodynamic data in the context of isocore nucleation. We have identified relevant data that will help to build isochoric cryopreservation protocols in the near future. There is a main series of cryopreservatives that are commonly used for which thermodynamic data and comparative tests have been generated for characterization in previous works: [47] [48] .

The means by which the study of the isochore nucleation phenomenon was carried out until recently were the physical quantities such as pressure and temperature through which the knowledge bases were laid that directed the studies and diversified the areas of interest. Until now, there has not been an isometric reactor with transparent walls that would open the horizon in a visual direction of study. This paper undertakes an experimental examination of water nucleation, using a specially designed isochore cylinder with transparent upper and lower sections. The use of an isometer cylinder in this context facilitates a controlled and restricted environment for investigation, with the transparency of the vessel allowing direct visual observation of nucleation phenomena throughout the experiment. The study revealed a perceptible prevalence of heterogeneously distributed nucleation zones in the limited volume of water. These areas manifested as localized regions where the transition from the liquid phase to the solid phase was initiated. By using advanced microscopic imaging techniques, the research successfully identified and characterized the spatial distribution of these nucleation zones. It is observed that the initiation of the nucleation process originates near the inner wall of the aluminum isochorus cylinder, following an anticipated pattern in which the nucleation events progress radially towards the central axis of the confined space. This result aligns with theoretical expectations, justifying the influence of container boundaries on nucleation site initiation and subsequent radial expansion. The observed nucleation dynamics conform to the established principles governing phase transitions in restricted environments, highlighting the spatially dependent nature of the nucleation phenomenon in the current experimental context. The growth dynamics of crystal structures were systematically examined, shedding light on the temporal evolution of nucleation events. Intriguingly, the study identified visually distinct features such as the formation of complicated dendritic structures, spatial heterogeneities in nucleation, and dynamic interactions between neighboring nucleation events. These unique visual features not only enrich our qualitative understanding of nucleation, but also provide a basis for further quantitative analyses, helping to refine theoretical models in the field.

The temporal evolution of water nucleation within the limits of the isochore cylinder constitutes a focal point of this experimental research and consists of three distinct phases: the initial phase, the early growth, the second aggregation and the maturation and balancing, the last phase. The beginning of temporal evolution is marked by the initiation of nucleation events near the inner surface of the isochore cylinder. The analysis in this phase reveals information about the role of heterogeneous nuclear zones and their spatial distribution along the reactor wall.

The practical implications of the study's findings provide insights into the control or manipulation of nucleation processes for specific applications (preservation of biological matter) or industries (food industry). Future directions for research based on gaps or unanswered questions identified in our visual study could include exploring different experimental conditions, incorporating additional variables, or refining visualization techniques.

Precise control of experimental conditions: the small size of the reactors allows for tighter and more precise control of experimental parameters, such as temperature, pressure and the nature of the substances being studied.

The need to increase the volume of reactors. As research advances and the knowledge gained requires validation on a larger scale, it becomes necessary to increase the volume of isochoric reactors. The main reasons for this scaling include: practical and industrial relevance, the practical application of research results requires large-scale testing.

We can conclude that although small isochoric reactors are ideal for early research due to their precise control, resource savings and increased safety, increasing the volume of these vessels is essential for the validation and practical application of the results obtained. Scaling enables complex problems to be addressed, the practical relevance of research and the expansion of processes at an industrial level.

11. CHAPTER 11: Own contributions, future directions in research and its limits

The scientific research methodology was experimental, based on multiple repetitions from which the experimental data were recorded, which were subsequently processed, analyzed, put in context and subsequently were the basis for the elaboration of scientific articles published in journals of international interest.

I will list the results obtained below in a random order:

- We started by deeply documenting the theme in the selected field, going through a large number of papers by accessing the bibliography and selecting the relevant and representative materials from which we started, resulting in the elaboration of the current stage of research, the basic chapter of this work.
- Participatory involvement in a research project won in a project competition (PNCDI III), called: "Study of thermodynamic profiles in isochoric regime for the most important

cryoprotective substances", project code: PN-III-P4-ID-PCE-2020-1706 associated with contract no. PCE2302021. Through the role of research assistant that I obtained following the competition to which I applied, within this project I had the opportunity to participate in the experimental studies that follow nucleation in the isochore environment, within an organized team, which ended with the publication of articles on the preservation at negative temperatures of small fruits (grapes) and on the liquid-solid balance of the cryopreservative Custodiol in isocore thermodynamic conditions at negative temperatures. I mention that a third article on the preservation of raspberries in isocrum is submitted for review to a specialized journal.

- The mathematical model presented in the designated chapter is based on a series of fundamental principles that are selected from the literature and describe at a fundamental level the thermodynamic processes in an isochore system.
- Conceptualization of a simulation model of phenomena inside a constant volume reactor, using specialized software for applications in the field of physics and engineering, which was completed with a paper published in IOP Conference Series: Materials Science and Engineering, ISSN-1757-899X.
- The concept and implementation of a completely new mechanical device, for visual studies in the isochore environment, with the possibility of controlling thermodynamic parameters, an original element, which was the basis of several studies in this work. Thus, a new experimental stand was created in the refrigeration laboratory of the Installations Department of the Faculty of Constructions of the Transilvania University of Brașov. This device can be used both for the continuation of studies in the field and for teaching purposes by students.
- The generation of novelties, data and concepts about the phenomenon of nucleation of water or other aqueous substances in the isochore were produced through experimental studies with measurements of temperature and pressure parameters, or using the microscope for the visual study of the phenomenon, recording image captures from inside a reactor with constant volume. The dissemination of the results was then achieved by publishing three papers in peer-reviewed journals: two in AIP Advances, ISSN 2158-3226 and one in Nature Scientific Reports ISSN 2045-2322.
- Obtaining multiple images from inside an isochoric reactor that would allow us to evaluate from a spatial point of view, or the actual dynamics during an experiment of freezing and thawing water in the isocor. These relevant novelties can answer questions such as: what is the frozen zone and which is the zone that remains liquid after nucleation? Or what can be the ideal position in an isochoric reactor to place biological material in order to preserve it in maximum safety conditions? Or how we can use nucleation triggers to propagate ice crystals around them, and the list goes on.

- Active involvement in experimental studies: from actual procedures, use of equipment, parameterization and control, to data collection, interpretation, writing of articles and their reviews. The activity was carried out together with the research team from the refrigeration laboratory in order to develop the constant volume cooling technique, resulting in the publication of articles in journals such as: Heliyon ISSN 2405-8440, Biochemical and biophysical research communications ISSN 0006-291X, Cryobiology ISSN-0011-2240, Bioengineering ISSN 2306-5354.
- I have been involved in 8 articles published so far, and the identification data and links can be found in the following list:
    1 Câmpean, ȘI., Bește, GA., Tăbăcaru, MB. et al. Revealing isochoric water nucleation: a visual study. Sci Rep 14, 10086 (2024). https://doi.org/10.1038/s41598-024-61053-y
    2 Ștefan I. Câmpean et al., "Liquid–solid equilibria and supercooling of Custodiol® in isochoric thermodynamic systems at subfreezing temperatures," Physics of Fluids, vol. 35, no. 10, Oct. 2023, https://doi.org/10.1063/5.0169216
    3 G. Năstase et al., "Isochoric Supercooling Organ Preservation System," Bioengineering, vol. 10, no. 8, Aug. 2023, https://doi.org/10.3390/bioengineering10080934
    4 Ștefan I. Câmpean et al., "Preservation of black grapes by isochoric freezing," Heliyon, vol. 9, no. 7, p. e17740, Jul. 2023, https://doi.org/10.1016/j.heliyon.2023.e17740.
    5 G. A. Bește et al., "Temperature-pressure correlations of cryoprotective additives for the design of constant volume cryopreservation protocols," Cryobiology, no. July, 2022, https://doi.org/10.1016/j.cryobiol.2022.08.001.
    6 Beschea GA , Campean SI , Tabacaru MB , Vutoiu BG , Serban A , Nastase G . A state of the art review of isochoric cryopreservation and cryoprotectants. Cryo Letters. 2022 Jul-Aug; 43(4):189-199. PMID: 36626122. https://pubmed.ncbi.nlm.nih.gov/36626122/
    7 G.-A. Bește, Ștefan-I. Câmpean, M.-B. Tăbăcaru, A. Șerban, B. Rubinsky, and G. Năstase, "Glucose and glycerol temperature-pressure correlations for the design of cryopreservation protocols in an isochoric system at subfreezing temperature," Biochem Biophys Res Commun, vol. 559, pp. 42–47, 2021, doi: https://doi.org/10.1016/j.bbrc.2021.04.084.
    8 G A Bește1, Ș I Câmpean1, L M Scutaru2, L Costiuc2 and A Șerban3, „Freezing water simulations in isochoric systems – preliminary analysis" https://iopscience.iop.org/article/10.1088/1757-899X/1138/1/012003
    9 S. I. Câmpean, G. A. Beschea, A. Serban, M. J. Powell-Palm, B. Rubinsky, and G. Nă stase, "Analysis of the relative supercooling enhancement of two emerging

supercooling techniques," AIP Adv, vol. 11, no. 5, May 2021, https://doi.org/10.1063/5.0051662.

As a further proposal regarding the direction of study after the experience gained from the elaboration of this documentation, I consider the following aspects relevant:

- Conducting an experiment of microscopic visualization of the phenomenon of nucleation and isochoral crystallization up to the triple point of water, using the same device specially created for visualization and then the inverse phenomenon of slow melting after reaching thermodynamic equilibrium
- Tracking a part of biological material placed in the isochore chamber and visualizing it during the isochore freeze.
- Use of a substance as a nucleation trigger for the visual study of behaviour and dynamics in such a context
- The use of mixtures of cryopreservatives instead of water and the visual study of their behavior under the microscope following the same experimental protocol used in the study of thermodynamic profiles
- Use and comparison of the 3 variable volumes of the isochore chamber and compare the dynamics of ice crystals according to the internal volume and shape of the isochore chamber.

In conclusion, we can say that the experimental studies presented in this paper have generated relevant information about the phenomenon of nucleation in isochorus regarding the random nucleation behavior, demonstrating the stability of the metastable state of water supercooling by means of the volume restriction technique compared to another technique that separated the air-water interface by means of a synthetic oil film, which had a good performance, comparable to the isochore, in terms of lowering the nucleation temperature point or the first images from inside an isochore reactor, photo and video materials with the nucleation trigger, the formation of ice crystals and then the reverse melting phenomenon and the dynamics of the frozen content inside. And last but not least, the study that generated thermodynamic data on Custodiol, a cryoprotective substance used in transplant medicine, under isochoric conditions, obtaining data such as: nucleation temperature or behavior in a metastable state of subcooling.

These novelties are unique and very valuable for future exploration of the field. Using both the concept of the visualization device and information on the dynamics of nucleation, more pieces were added to this large set of properties regarding the deepening of this theme.

12. LIST OF FIGURES AND TABLES

13. REFERENCES

[1] "F. Chiriac, Refrigeration Installations, Bucharest: Didactic and Pedagogical Publishing House, 1981".

[2] E. A. Gillispie, "An Examination of an Ice House at Old Town Plantation," 2012.

[3] by Brian Roberts and C. Heritage Group, "JOHN GORRIE and his ICE MACHINE."

[4] J. Gladstone, "John Gorrie, The Visionary," *ASHRAE J*, vol. 40, no. 12, pp. 29–35, 1998.

[5] Remus Răduleț et al., *Romanian Technical Lexicon, Bucharest: Technical Publishing House 1957-1966*.

[6] Șerban Țițeica, *Thermodynamics, Publishing House of the Academy of the Socialist Republic of Romania, Bucharest*, . 1982.

[7] A. Academy and A. Academy, "Water , in the Liquid and Five Solid Forms , under Pressure Author (s): P . W . Bridgman Source : Proceedings of the American Academy of Arts and Sciences , Vol . 47 , No . 13 (Jan ., Published by : American Academy of Arts & Sciences Stable URL : http," vol. 47, no. 13, pp. 441–558, 2017.

[8] E. B. Moore and V. Molinero, "Structural transformation in supercooled water controls the crystallization rate of ice," *Nature*, vol. 479, no. 7374, pp. 506–508, 2011, doi: 10.1038/nature10586.

[9] B. J. Murray and A. K. Bertram, "Formation and stability of cubic ice in water droplets," *Physical Chemistry Chemical Physics*, vol. 8, no. 1, pp. 186–192, 2006, doi: 10.1039/b513480c.

[10] T. M. Gasser, A. V. Thoeny, A. D. Fortes, and T. Loerting, "Structural characterization of ice XIX as the second polymorph related to ice VI," *Common Nat*, vol. 12, no. 1, 2021, doi: 10.1038/s41467-021-21161-z.

[11] M. J. Powell-Palm and B. Rubinsky, "A shift from the isobaric to the isochoric thermodynamic state can reduce energy consumption and augment temperature stability in frozen food storage," *J Food Eng*, Vol. 251, no. August 2018, pp. 1–10, 2019, yogurt: 10.1016/j. jfudeng.2019.02.001.

[12] M. J. Powell-Palm, A. Koh-Bell, and B. Rubinsky, "Isochoric conditions enhance stability of metastable supercooled water," *Appl Phys Lett*, vol. 116, no. 12, Mar. 2020, doi: 10.1063/1.5145334.

[13] J. H. Topps and R. C. Elliott, "© 1965 Nature Publishing Group," *Nature Publishing Group*, vol. 205, no. 5007, pp. 498–499, 1965.

[14] R. Chow, R. Blindt, R. Chivers, and M. Povey, "A study on the primary and secondary nucleation of ice by power ultrasound," *Ultrasonics*, vol. 43, no. 4, pp. 227–230, 2005, doi: 10.1016/j.ultras.2004.06.006.

[15] S. A. Szobota and B. Rubinsky, "Analysis of isochoric subcooling," *Cryobiology*, vol. 53, no. 1, pp. 139–142, Aug. 2006, doi: 10.1016/j.cryobiol.2006.04.001.

[16] L. Hawkes, "Super-cooled water [2]," *Nature*, vol. 124, no. 3119, pp. 225–226, 1929, doi: 10.1038/124225b0.

[17] B. J. Murray, D. O'sullivan, J. D. Atkinson, and M. E. Webb, "Ice nucleation by particles immersed in supercooled cloud droplets," *Chem Soc Rev*, vol. 41, no. 19, pp. 6519–6554, 2012, doi:10.1039/c2cs35200a.

[18] A. N. Consiglio, D. Lilley, R. Prasher, B. Rubinsky, and M. J. Powell-Palm, "Methods to stabilize aqueous supercooling identified by use of an isochoric nucleation detection (INDe) device," *Cryobiology*, no. March, 2022, doi: 10.1016/j.cryobiol.2022.03.003.

[19] Y. Zhao, L. Lou, C. Lyu, M. J. Powell-Palm, and B. Rubinsky, "Isochoric supercooling cryomicroscopy," *Cryobiology*, 2022, doi: 10.1016/j.cryobiol.2022.02.002.

[20] B. Rubinsky, P. A. Perez, and M. E. Carlson, "The thermodynamic principles of isochoric cryopreservation," *Cryobiology*20, Vol. 50, No. 2, pp. 121–138, 2005, doi: 10.1016/j. Cryobiol.2004.12.002.

[21] P. D. Sanz, L. Otero, C. De Elvira, and J. A. Carrasco, "Freezing processes in high-pressure domains," *International Journal of Refrigeration*, vol. 20, no. 5, pp. 301–307, 1997, doi: 10.1016/S0140-7007(97)00027-3.

[22] L. Ter Minassian, P. Pruzan, and A. Soulard, "Thermodynamic properties of water under pressure up to 5 kbar and between 28 and 120 °C. Estimations in the supercooled region down to -40 °C," *J Chem Phys*, vol. 75, no. 6, pp. 3064–3072, 1981, doi: 10.1063/1.442402.

[23] "Material properties - aluminum alloy," https://www.makeitfrom.com/material-properties/7075-T6-Aluminum.

[24] Ltd. Precision Sapphire Technologies, "Material Properties - Sapphire."

[25] H. Huang, M. L. Yarmush, and O. B. Usta, "Long-term deep-supercooling of large-volume water and red cell suspensions via surface sealing with immiscible liquids," *Common Nat*, vol. 9, no. 1, p. 3201, Aug. 2018, doi: 10.1038/s41467-018-05636-0.

[26] S. I. Câmpean, G. A. Beschea, A. Serban, M. J. Powell-Palm, B. Rubinsky, and G. Nă stase, "Analysis of the relative supercooling enhancement of two emerging supercooling techniques," *AIP Adv*, vol. 11, no. 5, May 2021, doi: 10.1063/5.0051662.

[27] Y. Zhao, L. Lou, C. Lyu, M. J. Powell-Palm, and B. Rubinsky, "Isochoric supercooling cryomicroscopy," *Cryobiology*, 2022, doi: 10.1016/j.cryobiol.2022.02.002.

[28] M. J. Powell-Palm, B. Rubinsky, and W. Sun, "Freezing water at constant volume and under confinement," *Common Phys*, vol. 3, no. 1, 2020, doi: 10.1038/s42005-020-0303-9.

[29] Ștefan I. Câmpean, G. A. Beșchea, M. B. Tăbăcaru, and G. Năstase, "Revealing isochoric water nucleation: a visual study," *Ski Rep*, vol. 14, no. 1, pp. 1–12, 2024, doi: 10.1038/s41598-024-61053-y.

[30] C. Bilbao-Sainz *et al.*, "Preservation of spinach by isochoric (constant volume) freezing," *Int J Food Sci Technol*, vol. 55, no. 5, pp. 2141–2151, 2020, doi: 10.1111/ijfs.14463.

[31] B. R. Chenang Lyu, Gabriel Nastase, Gideon Ukpai, Alexandru Serban, "A comparison of freezing-damage during isochoric and isobaric freezing of the potato," *PeerJ*, 2017, doi: 10.7717/peerj.3322.

[32] R. Dhanya, A. Panoth, and N. Venkatachalapathy, "A comprehensive review on isochoric freezing: a recent technology for preservation of food and non-food items," *Sustainable Food Technology*, vol. 2, no. 1, pp. 9–18, 2023, doi: 10.1039/d3fb00146f.

[33] C. Bilbao-Sainz *et al.*, "Preservation of grape tomato by isochoric freezing," *Food Research International*, vol. 143, no. February, p. 110228, 2021, doi: 10.1016/j.foodres.2021.110228.

[34] Y. You, T. Kang, and S. Jun, "Control of Ice Nucleation for Subzero Food Preservation," *Food Engineering Reviews*, vol. 13, no. 1. Springer, pp. 15–35, Mar. 01, 2021. doi: 10.1007/s12393-020-09211-6.

[35] T. G. Rinwi, J. Ma, and D.-W. Sun, "Effects of isochoric freezing on myofibrillar protein conformational structures of chicken breasts," *LWT*, vol. 181, p. 114768, May 2023, doi: 10.1016/j.lwt.2023.114768.

[36] Ștefan I. Câmpean *et al.*, "Preservation of black grapes by isochoric freezing," *Helion*, vol. 9, no. 7, p. e17740, Jul. 2023, doi: 10.1016/j.heliyon.2023.e17740.

[37] C. Bilbao-Sainz *et al.*, "Preservation of sweet cherry by isochoric (constant volume) freezing," *Innovative Food Science and Emerging Technologies*, vol. 52, pp. 108–115, Mar. 2019, doi: 10.1016/j.ifset.2018.10.016.

[38] D. F. Bridges *et al.*, "Viability of Listeria monocytogenes and Salmonella Typhimurium after isochoric freezing," *J Food Saf*, vol. 40, no. 5, pp. 1–8, 2020, doi: 10.1111/jfs.12840.

[39] M. J. Powell-Palm, J. Preciado, C. Lyu, and B. Rubinsky, "Escherichia coli viability in an isochoric system at subfreezing temperatures," *Cryobiology*, vol. 85, pp. 17–24, Dec. 2018, doi: 10.1016/j.cryobiol.2018.10.262.

[40] H. Mikus, A. Miller, G. Nastase, A. Serban, M. Shapira, and B. Rubinsky, "The nematode Caenorhabditis elegans survives subfreezing temperatures in an isochoric system," *Biochem Biophys Res Common*, vol. 477, no. 3, pp. 401–405, 2016, doi: 10.1016/j.bbrc.2016.06.089.

[41] G. Năstase, C. Lyu, G. Ukpai, A. Șerban, and B. Rubinsky, "Isochoric and isobaric freezing of fish muscle," *Biochem Biophys Res Common*, vol. 485, no. 2, pp. 279–283, Apr. 2017, doi: 10.1016/j.bbrc.2017.02.091.

[42] C. Bilbao-Sainz *et al.*, "Preservation of Tilapia (Oreochromis aureus) Fillet by Isochoric (Constant Volume) Freezing," *Journal of Aquatic Food Product Technology*, vol. 29, no. 7, pp. 1–12, 2020, doi: 10.1080/10498850.2020.1785602.

[43] M. Powell-Palm, J., V. Charwat, B. Charrez, B. Siemons, E. K. Healy, and B. Rubinsky, "Isochoric supercooled preservation and revival of human cardiac microtissues," *Biol Common*, vol. 4, p. 1118(2021), 2021.

[44] L. Wan *et al.*, "Preservation of rat hearts in subfreezing temperature isochoric conditions to – 8°C and 78MPa," *Biochem Biophys Res Common*, vol. 496, no. 3, pp. 852–857, Feb. 2018, doi: 10.1016/j.bbrc.2018.01.140.

[45] G. Năstase *et al.*, "Isochoric Supercooling Organ Preservation System," *Bioengineering*, vol. 10, no. 8, Aug. 2023, doi: 10.3390/bioengineering10080934.

[46] M. J. Powell-Palm *et al.*, "Cryopreservation and revival of Hawaiian stony corals using isochoric vitrification," *Common Nat*, vol. 14, no. 1, p. 4859, Aug. 2023, doi: 10.1038/s41467-023-40500-w.

[47] G. A. Beșchea *et al.*, "Temperature-pressure correlations of cryoprotective additives for the design of constant volume cryopreservation protocols," *Cryobiology*, no. July, 2022, doi: 10.1016/j.cryobiol.2022.08.001.

[48] G.-A. Beșchea, Ștefan-I. Câmpean, M.-B. Tăbăcaru, A. Șerban, B. Rubinsky, and G. Năstase, "Glucose and glycerol temperature-pressure correlations for the design of cryopreservation protocols in an isochoric system at subfreezing temperature," *Biochem Biophys Res Common*, vol. 559, pp. 42–47, 2021, doi: https://doi.org/10.1016/j.bbrc.2021.04.084.